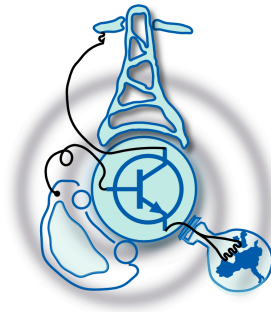# Train mechanical - kinematic modeling and control for traction network analysis

by

Ha, Ngoc Hieu

Submitted to the Department of Electrical Engineering, Electronics, Computers and Systems
in partial fulfillment of the requirements for the degree of

Master in Electrical Energy Conversion and Power Systems

at the

UNIVERSIDAD DE OVIEDO

July 2016

© Universidad de Oviedo 2016. All rights reserved.

Author . . . .

Certified by . . . .
Pablo Arboleya Arboleya
Associate Professor
Thesis Supervisor

Train mechanical - kinematic modeling and control for traction network analysis

by

Ha, Ngoc Hieu

Abstract

Modern railways systems nowadays has been subjected to extensive research and development. Researchers' attention are increasingly paid to various topics ranging from planning and operation of the whole traction network to more specific aspects of the train itself such as train trajectory, predictive control, train stop control, braking strategy, etc. Whether the focus is on a bigger scale of energy management to a local scale of different algorithms for automatic train operation (ATO), the ultimate goal is to optimize the aspects of energy efficiency, punctuality and passenger comfort. The first step to such a big chain of researches is to model the mechanical - kinematic behavior of the train as well as to figure out how the train is controlled with respect to time, speed and distance. This master thesis will firstly cover a review of train model, afterwards a number of control loops will be implemented and simulated by Matlab. Different conditions of the railroad and various constraints in train's characteristic parameters will be taken into account when simulating the model and discussed thereafter. Though not necessarily being state of the art of train control, the simulator is useful for characterizing the mechanical behavior of the train, whose resulting variables will be integrated into a traction network solver to verify and form a full train traction system simulation towards the later part of the thesis. Since the power flow electric solver is very complex, the goal of the thesis is to have a fast and simple train simulators, rather than very accurate and using complicated algorithms.

Thesis Supervisor: Pablo Arboleya Arboleya
Title: Associate Professor

Acknowledgments

For my master study and this thesis in particular to be completed, I would like to express special thanks to all the professors who have taught me in all the courses for their guidance, especially professor Pablo Arboleya Arboleya, who is the supervisor of this thesis. Besides, I would also like to thank my family and friends for their support which give me great encouragement during the whole master course.

Contents

List of Figures

List of Tables

Chapter 1

Introduction to train modeling and control

Like other sectors, global saving in energy has becoming crucial in transportation sector for years. Among them, railway is always an essential mean of transportation which has the advantage of economic cost as well as the unique reliability and punctuality. As the result, massive research and developments have been made on the railway system, which comprises of various interesting topics in itself. As the electrification of trains has been firmly replacing the diesel locomotive counterpart due to its environmental friendliness and high energy efficiency, researchers and engineers nowadays are trying to optimize the railways traction network through different aspects such as the power supply network or the train control methodology. Like any other problem, the first step of all these studies is to model the controlled object, which is the train in this case. Several existing train models in literature are presented in the the first section of chapter 1. Afterwards, different train control problems will also be reviewed in the second sections, among which the basic control scheme will be the focus point of the thesis.

Details of the chosen train model and the control algorithms including speed control loop, sole distance control loop and cascade control will be presented in chapter 2. The modeling and control will be implemented based on Matlab environment.

Next, chapter 3 will discuss the train simulation results and comment on important

aspects regarding the performance of the control schemes.

Finally, chapter 4 will integrate the result obtained from the train simulation with the electric traction network solver developed in other work to form a complete railways traction system simulation.

1.1 Train modeling review

1.1.1 Single mass model

The most common and prevalent train model used among researchers is the single mass model due to its clear physical principle. It is generally based on the second Newton's law applied to one object and can be briefly summed up below:

$$
\begin{cases}
\dfrac{ds}{dt} = v \\
m\dfrac{dv}{dt} = F - R(s,v)
\end{cases}
\tag{1.1}
$$

where s is the traveled distance or the position of the train, v is the the speed, F is the controlled traction or braking force, and R represents different kinds of resistances including rolling resistance between the train and the rail roads, the aerodynamic resistance that depends on the train speed and the resistance upon railroad characteristics such as the gradient and the curvature. To be more general, some papers also consider the rotating mass to the equation, multiplying a factor of ρ to the mass of the train [1]-[3].

There is another variation of these equations where the authors want to relate directly the position and the speed of the train as following [4]-[5]:

$$
\begin{cases}
\dfrac{dt}{ds} = \dfrac{1}{v} \\
m\dfrac{dv}{ds} = \dfrac{F - R(s,v)}{v}
\end{cases}
\tag{1.2}
$$

Either way, the controlled variable F, in most of the cases, is directly derived from the speed control of the train. This will be the model used in this thesis and the

details of the equation's elements will be clearly illustrated in the next chapter.

1.1.2 Cascade mass model

For heavy haul train modeling, a cascade mass model brings a better representation of the internal dynamic of the train. The interaction forces between adjacent cars can change the whole picture with the possibility of more energy waste and train damages. The cascade mass model considers the train as a string of masses, which normally represents the train's cars. The general equations for this model can be expressed as following [6]-[7]:

$$
\begin{cases}
\dot{x}_i = v_i - v_{i+1}, i = 1, ..., n-1 \\
m_i \dot{v}_i = F_i + F_{in_{i-1}} - F_{in_i} - R_i, i = 1, ..., n
\end{cases}
\tag{1.3}
$$

where m_i and v_i are the mass and speed of the ith car, respectively. x_i is the relative displacement between the ith and the (i-1)th car. F_i is again the controlled force, either the traction or braking force. R_i denotes all the resistances act on the ith car, including sources of rolling resistance, aerodynamics, gradient and curvature. F_{in_i} is the in-train forces between the ith and the (i+1)th car, allowing to study the internal interaction of the train. F_{in_i} normally is a function of the displacement as well as the difference in speed of two successive cars, which can be written as:

$$
F_{in_i} = k_i x_{in_i} + d_i \dot{x}_{in_i}, F_{in_0} = F_{in_n} = 0
\tag{1.4}
$$

It can be seen that the optimization problem would face difficulty due to the non-linearity of equation (1.3) brought by the presence of v^2 and other terms not dependent on v. [7] proposes a linearized model by neglecting the damping effect d in (1.4) and introducing a new controlled variable $F_i' = F_i - R_i'$ that group all the elements in the resistance forces that cause non-linearity to the equation into R_i'. Details of related algorithms, however, will not be further mentioned here to avoid digression. Applications of the studies based on cascade mass model can be seen in

mentioned references. Block diagram and forces diagram of the cascade model are shown in Figure 1-1 (with forces in other direction than the traveling path not shown).
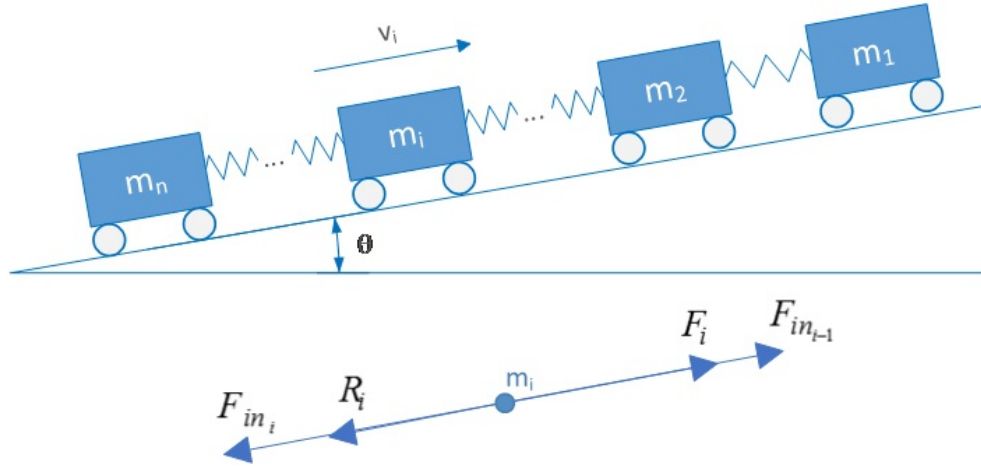
Figure 1-1: Block diagram of cascade mass model and forces diagram acting on one mass (only forces in or opposite to traveling direction are shown).

1.1.3   Other models

In [8], the train was considered as a **black box** - an unknown system and characterized by interpolation and curve fitting from the acquired data through the on-board monitoring system, which include the absorption and traction data. Using genetic algorithm, its objective function can be expressed by:

$$F(t_1, ..., t_7) = E(t_1, ..., t_7) \times T_{tot} \tag{1.5}$$

where $t_1, ...t_7$ are the intervals for each traction condition, defined as: Maneuver, Series, Parallel, Reduced Field 1, Reduced Field 2, Reduced Field 3, and Coasting. $E(t_1, ..., t_7)$ is the energy consumption obtained from measurement data and T_{tot} is the total trip time. Genetic algorithm is a method used for optimization of system with or without constraints, based on the biological natural selection [8]. The optimization goal, in this case, is to jointly minimize the trip time and the consumption.

In another study, [9] uses a **fuzzy model** to implement a train control optimizing the energy conservation, passenger comfort and traveling time. Such a model is based

on a multiple input - single output scheme: If U_1 is B_{i1} AND U_2 is B_{i2} AND ... AND U_r is B_{ir} THEN V is D_i, where $i = 1, ..., m$ is the number of rules and r is the number of inputs. B_{ij} and D_i are the membership functions of the inputs and outputs. This type of modeling also uses the data obtained from the train to create a dynamic model. The use of fuzzy modeling technique are also used in [10]-[11] in development of automatic train operation control.

1.2   Control problems

Generally in a railway systems, there are two main sub-systems that need to be managed and controlled: the train itself which normally includes the traction machine, and the electrical traction network. In literature, these two parts are often decoupled and studied separately. In this thesis, the subject also center on the train system only, with the kinematic modeling and simulation of the train. The electric simulator of the traction network will also be mentioned towards the last chapter, before being coupled with the train simulator to check the solver operation.

Regarding particularly the train control problems, there are a number of main research topics. The most popular one is the study of optimal trajectory for trains, either controlled by the driver or the automatic train operation (ATO). This is normally modeled as an optimization problem with a range of objectives such as energy efficiency, punctuality, riding comfort, train stop accuracy. The methods used for such an optimization problem can be maximum principle based, heuristic, dynamic programming, or sequential quadratic programming methods. Most of the time the optimal speed profile is realized in acceleration - constant speed - cruising - deceleration sequence. Examples of these studies can be seen in [2], [3], [16]-[27]. Among that, the train stop control and the braking strategy with regenerative capability can also be big problems by themselves. In an ideal and simple train network, the train operator or the ATO system will follow the calculated speed profiles (usually in a form of speed curve vs position), which can be along the whole distance between two stations or on local sections divided based on the track characteristics, and punctual-

ity is normally achieved. However in a complex systems, conflicts may arise anytime not only from the train itself but also from other trains in a busy network or from traction grid disturbances and constraints. That leads to the requirement to have real time control, somehow updating the control action to compensate for the deviation or to completely solve a new optimization problem in real time to adjust the speed profile. This scheduling problem has been solved under methods such as using predictive model predictive control, branch and bound algorithm, tabu search, Lagrangian heuristic, genetic algorithm, differential evolution, simulation, etc [28]-[37].

1.3   Objective of the thesis

In another work, a railway electric traction network was modeled and simulated to solve the power flow problem of the system. The trains are considered as moving loads, with both position and power changing over time. In order to simulate a complete system, we need a train simulation which gives the train position and power as the result. This motion cannot be arbitrary or too simple (such as a train running with constant speed), but has to resemble the motion of real trains as much as possible. Moreover, a simulation platform has to be implemented such that it has capability to simulate any custom motion needed (ie., changes in trajectory, track condition, etc). Therefore, a train control that simulates the behavior of either the driver or the ATO system is going to be done in this thesis.

Those optimal control schemes mentioned previously, however, is not the focus of the thesis. In this study, since the goal is only to characterize the motion and consumption of a train in order to integrate it with the electric traction network, we will use classic PID control schemes with the speed or the position as the main control variable having a preset trajectory versus time. The electric simulator is generally rather complex, therefore we want the train simulator to be fast and simple, instead of using state of the art algorithm and producing very accurate simulation. Three control strategies will be proposed and implemented. Results obtained by simulation will be compared among three strategies. Details of the control schemes will be

elaborated in a later part.

Eventually, the resulting data from the train simulator will be passed to the electric simulator to complete the whole railways traction network simulation. Effect of each control strategies will also be looked at. The purpose of this integration, in the scope of this thesis, is only to check the basic operation of the electric solver. Therefore, no further consideration is paid to real time operation affecting aspects such as voltage constraint or train over current protection.

Chapter 2

Single mass modeling and controlling schemes

2.1 The model

2.1.1 The equation

As mentioned in chapter 1, in this thesis we will use the single mass model, whose diagram is depicted in Figure 2-1. The resistance forces in R from equation 1.1 includes:

- F_r: the basic resistance,

- F_c: the resistance generated by the railroad curvature,

- F_w: the resistance due to the weight of the train in a given gradient (which can be negative or positive),

- F_f: the rolling friction between the train and the railways.

The rolling friction is drawn separately only to illustrate the position at which it is generated. Normally in literature and hereafter, it is grouped into the basic resistance F_r, which also includes the aerodynamic resistance and internal mechanical resistances.
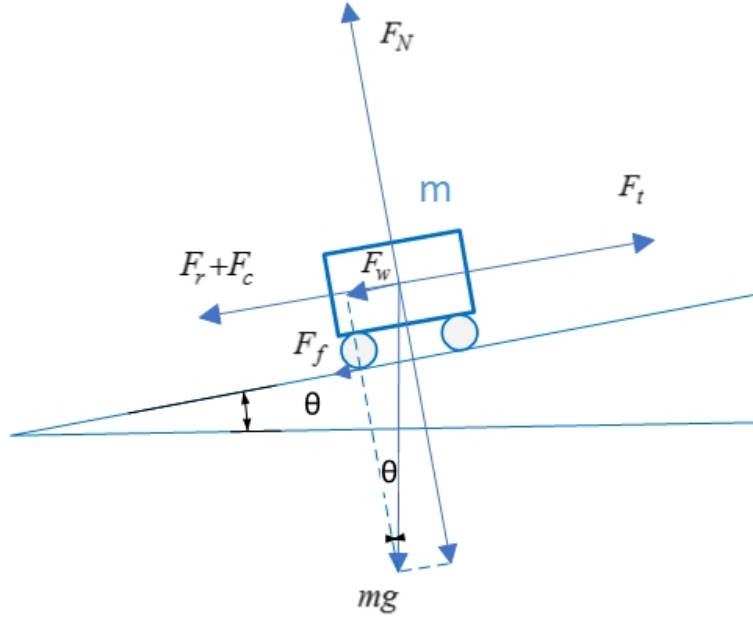
Figure 2-1: Single mass model force diagram

The Newton's second law equation applied to the model can be re-written as:

$$m\frac{dv}{dt} = F_t - F_r - F_c - F_w \tag{2.1}$$

Basic resistance The basic resistance is usually calculated by the "Davis equation" [12] which takes the form of:

$$F_r = A + Bv + Cv^2 \tag{2.2}$$

where A, B, C are empirical coefficients. A and B depends hugely on the mass as well as the vehicle characteristic and represent the rolling friction with the track and mechanical resistance from internal sources such as shaft rotation, transmission chain, which dominate when the train is running at low speed. Meanwhile, C is the coefficient relating to aerodynamic force, which becomes larger and more important when the speed increases. This equations is used in the condition of open air. While going in a tunnel, the train is subjected to additional resistance, which can be calculated by adding a factor k to the air resistance term Cv^2. A complete analysis of these coefficients can be found in [13]-[14].

Curvature resistance When traveling along a curvy track, the train experiences a resistance generated from the curvature nature. This resistance is quite complex to develop a theoretical calculation method, since it depends on not only the curve, but also the track characteristic, the train's mass and speed, the wheel distances, etc. An empirical way is used commonly to calculate such a resistance, which is expressed as following [15]:

$$F_c = m\frac{D}{1000r} \tag{2.3}$$

where m is the train mass (in kg), r is the radius of the curvature (in m) and D is the empirical coefficient which usually takes the value of 500 to 1200.

Weight resistance (or gradient resistance) This resistance originates from the gravity force acting on the train when it travel on a gradient surface. Although it is called "resistance", it can have the "traction" effect when the train is going down the slope. By convention, the weight resistance takes the positive value when going up the slope as depicted in Figure 2-1, and hence has to be subtracted in the sum of forces in equation 2.1. Also in Figure 2-1, this resistance, or the component of the gravity force that is in parallel with the surface, can be easily calculated as:

$$F_w = mgsin\theta \tag{2.4}$$

where g is the gravitational acceleration ($9.8m/s^2$).

2.1.2 Modeling constraints

The operation of the train is subjected to various constraints, both natural and artificial. Apparently, the power and traction force that can apply to the locomotive is limited to the electric machine characteristics, and so does the braking force when no special algorithm regarding regenerative braking is considered, which is the case in this thesis. Additionally, due to regulation, safety and passenger comfort, the train also have speed limit depending on the section of the track, as well as the limit in acceleration and jerk. We are going to look at each of these constraints in this section.

Traction machine limitation An example of the power and traction/braking force curves versus speed of a traction machine is shown in Figure 2-2[38]. This is
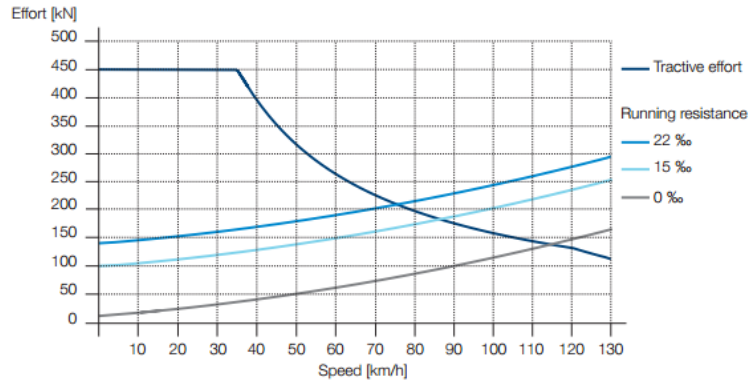
Figure 2-2: An example of traction force curve versus speed from ABB motors and generators.

similar to the power/torque - speed curves, as we can observe that there are two distinct operating regions: constant force and constant power. Below (normally) the rated speed, the maximum traction force the machine can generate is limited to a value. At higher speed, there will be a maximum power that can be extracted, and the traction force we can get out of the machine will be lower as the speed increases. There is also adhesive constraints between the train's wheels and the track that can limit the maximum possible traction force applied without making it skidding. However in this simulation, we will just assume the maximum traction force that can be extract from the electric machine is the higher value and will be used as the corresponding parameter.

Motion related constraints The three constraints related to train motion are the speed, acceleration and jerk. Due to safety regulation, every train have some speed limits that cannot be breached. Depending on different condition of sections of track, these limits may vary. For instance, speed limit in urban areas is often lower than that in country sides. Moreover, in order to smoother the train operation and enhance safety and passenger comfort, the acceleration and jerk (rate of change of acceleration) are also usually limited.

2.1.3 The complete model

In order to simulate the train motion on Matlab environment, we will divide a trip time into a string of small time intervals $\Delta t = t_{k+1} - t_k$. All of the variables will then be an array of discrete values, with the assumption that they remains constant during each interval. The main equations, therefore, will be expressed as:

$$ma_k = F_{t_k} - F_{r_k} - F_{c_k} - F_{w_k} \qquad k = 1, 2, 3, ... \tag{2.5}$$

From the acceleration, we can compute the corresponding velocity, position (or distance traveled) and jerk using following kinematic equations:

$$v_{k+1} = v_k + a_k \Delta t \qquad k = 1, 2, 3, ... \tag{2.6}$$

$$d_{k+1} = d_k + v_k \Delta t + \frac{1}{2} a_k \Delta t^2 \qquad k = 1, 2, 3, ... \tag{2.7}$$

$$\dot{j}_k = \frac{a_k - a_{k-1}}{\Delta t} \qquad k = 2, 3, 4, ... \tag{2.8}$$

Finally, the set of constraints that need to be taken into account are as following:

$$P_k < P_{max} \qquad k = 1, 2, 3, ... \tag{2.9}$$

$$F_{t_k} < F_{t_{max}} \qquad k = 1, 2, 3, ... \tag{2.10}$$

$$v_k < v_{max_k} \qquad k = 1, 2, 3, ... \tag{2.11}$$

$$a_k < a_{max_k} \qquad k = 1, 2, 3, ... \tag{2.12}$$

$$\dot{j}_k < \dot{j}_{max_k} \qquad k = 2, 3, 4, ... \tag{2.13}$$

2.2 Control schemes and implementation

2.2.1 Speed control

The most essential of any train control algorithm is the speed control. As mentioned before, more often than not, the speed profile will be developed beforehand as an optimization problem with various objectives such as energy saving, punctuality, passenger comfort. Based on the predefined speed, either the driver or the automatic control in an ATO system will try to follow the commanded speed, although in ATO equipped trains there is still often an operator on it for unplanned and emergence situations. Most of the time in literature, the speed profiles is expressed as a curve versus position. In this thesis, we will control it as a function of time. The closed loop control scheme can be demonstrated in Figure 2-3.
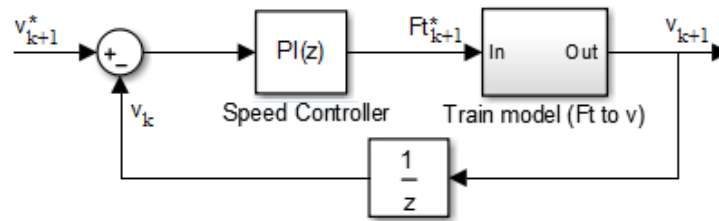
Figure 2-3: Train speed control scheme

2.2.2 Distance/Position control

Normally, the speed profile already implicitly integrates the time factor, ie. if the train follows exactly the speed command at any given position (in case of speed profile vs position) or at any given moment (in case of speed profile vs time) then it will achieve punctuality. Eventually, train speed control is only an intermediate mean to make sure the train follows the schedule, or in other words, the train complete a certain distance after a pre-scheduded time interval. Therefore, we can also implement another rather direct way to control the train motion, which has distance as the main controlled variable.

There are two possible control schemes based on distance. One is a cascade scheme

having distance control as the outer loop and speed control as the inner loop. The other is a sole distance control loop, with the controller output giving directly the commanded traction force. In both of the cases, the distance controller can be simply a proportional controller, since internally from speed to traveled distance we already have an integrator. The two control schemes are shown in Figures 2-4 and Figure 2-5.
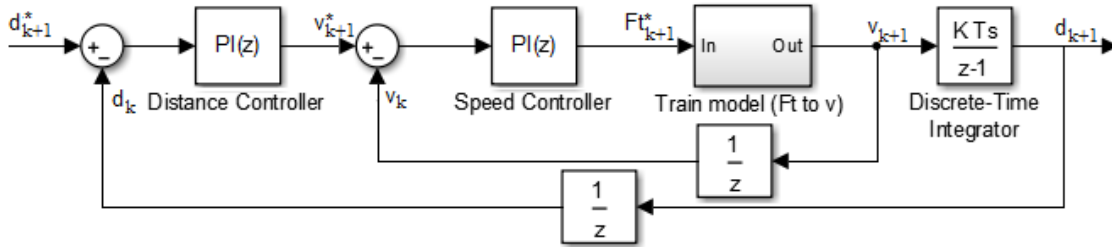
Figure 2-4: Cascade control scheme
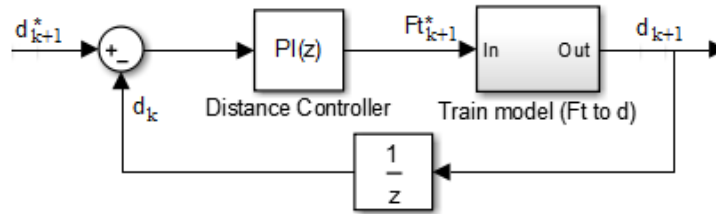
Figure 2-5: Sole distance control scheme

2.2.3   Trajectory generating scheme

In order to simulate the above control schemes, a preset trajectory of speed and distance versus time have to be defined. In order to do so, we will use the scheme illustrated in Figure 2-6. In this scheme, the speed reference at any instance will be calculated as the average speed needed to complete the rest of the distance in the amount of time left in the schedule. Note that the trip here is not necessarily the whole distance between two stations, hence no special care is paid to train stop control. This scheme is used solely for generating an example of train trajectory to apply to the simulation, not for real train control since there is no optimization implemented. However, all the constraints regarding power, traction force, speed, acceleration and jerk are still in place in order not to get an unpractical trajectory.

29
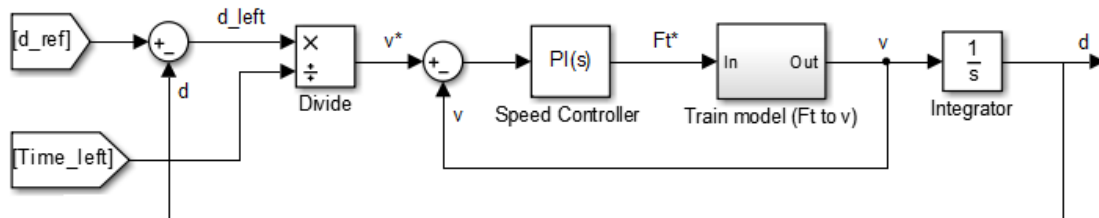
Figure 2-6: Trajectory generating scheme

Chapter 3

Simulation and discussion

3.1   Simulation platform and data

To simulate the train and its motion control, we will use Matlab environment. Apparently, all the train equations as well as the controllers are treated in discrete system manner (in which the PI controllers are expressed via Tustin method). It is important to note that the order of code blocks regarding the constraints has to be the motion limits first and the traction force, power limits follow. That way, we ensure the physical limits of the traction machine have final say in the event of conflicts among constraints. For example, when the train go up a hill, it will initially decelerate and the acceleration (possibly the jerk as well) reaches the negative limit. Meanwhile, to avoid such a quick decrease of speed, we need to apply more traction force, which can also reach the upper limit of the traction machine. In these cases, obviously the traction force/power constraints decide the next state of the system.

Another practical additional code block is the dead zone before every controller, which basically pass the error only when it's outside a threshold range, otherwise the error is considered to be negligible and the input to the controller will be set to zero. This is a mean to make stable the operation of the controllers, avoiding unnecessary oscillation when the error is near zero. For speed control scheme , this threshold is set to under 0.1km/h and for distance controls it is under 0.1m. The full Matlab script is attached along with the delivery of this thesis.

The parameters used for the train simulator are shown in Table.1. These are the set of values chosen based on popularity in literature as well as from typical light rail trains. They are defined at the beginning of the code, before each of the control schemes can be simulated separately. Among the resistances, the curvature and weight forces are shared among all control schemes, so they are declared in the parameter definition section. Meanwhile, due to the dependency on train speed, the basic resistance will be calculated in each of the control scheme sections and inside the iteration loop.

Since the simulation does not focus on local optimization of the speed profile, we will simply use one speed limit for the whole simulated trip. Also for simplicity, we will assume the train has the same braking capability as the traction capability, and there is a regenerative mechanism available on the train. Regarding the track conditions, a set of parameters are chosen randomly to create a few uphill and downhill as well as several curvy track sections. It is also important to note that the PI controllers' parameters are tuned manually by trials and based on the particular set of chosen data of the train system. These PI controller resembles the behavior of the train driver or the ATO system, which tries to regulate the speed (directly or indirectly) in order to meet the trajectory profile. Different parameters for the PIs will yield different motion behavior of the train. In this thesis, it is clear that the train equation described previously is non linear, hence an optimal tuning is not possible. However, by trials we will choose the most appropriate set of parameters in order to optimize the tracking performance of the controllers.

Table 3.1: Train parameters

Parameters	Values
Sampling frequency	$10Hz$
Train mass	$100000kg$
Curvature resistance coefficient D	800
Gravitational acceleration	$9.8m/s^2$
Basic resistance coefficient A	3000
Basic resistance coefficient B	80
Basic resistance coefficient C	20
Maximum speed	$100km/h$
Maximum/minimum acceleration	$\pm1m/s^2$
Maximum/minimum jerk	$\pm0.5m/s^3$
Maximum traction/braking force	$\pm450000N$
Maximum power consumption/regeneration	$\pm4500000W$

3.2   Simulation result

The Matlab scripts is designed to be run by sections of codes. After parameter definitions, the trajectory generating code will be run before each control schemes can be simulated separately. The control schemes can be run without any particular order, as long as they have enough data defined from the first two sections of codes.

Firstly and also randomly, the trajectory is generated so that the distance of 5km is completed in 870 seconds or 14.5 minutes. Again, this is not an optimization study, so there is no restriction of initial and final speed of the train in the section. In this case, we will just consider the train starts from zero speed and complete the section of 5km with whatever speed the scheme generates. The trajectory in terms of speed and traveled distance curves versus time are shown in Figure 3-1. Though not so important within the purpose of this trajectory generating simulation, other related curves including consumed/regenerated power, traction/braking force, acceleration, jerk and the resistance forces are also shown in Figure 3-1, 3-2, 3-3 for the completeness of the result. If the control variables in each of the control scheme manage to track the reference, the other related curves will also follow the general pattern (although not necessarily the exact curve).

33
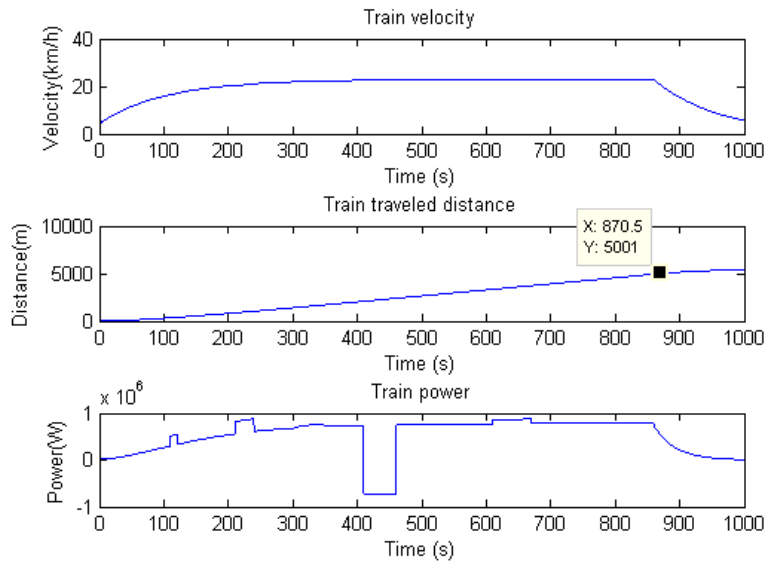
Figure 3-1: Generated speed, distance curves and power consumed/regenerated
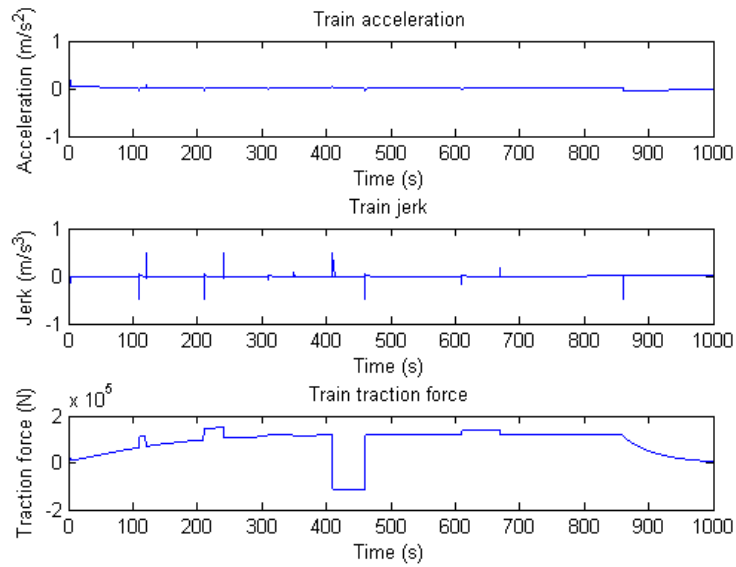
Figure 3-2: Train acceleration, jerk and traction/braking force using trajectory generating scheme
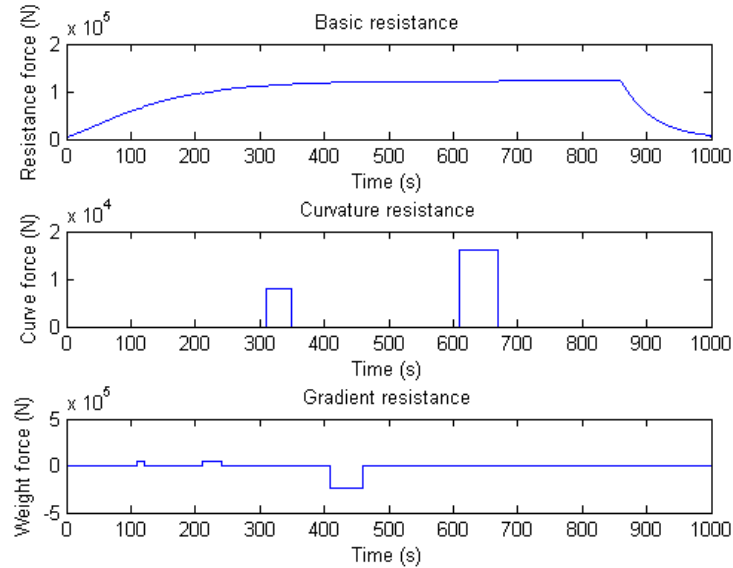
Figure 3-3: Resistance forces during the trip

As we can see, the generating scheme works quite well and the train completes the scheduled trip on time. The speed profile and the position trajectory will then be passed to appropriate control schemes as arrays of reference. We will look into the resulting simulation curves of every control scheme hereafter.

Speed control simulation   Firstly, we will have a look at the simulation result using speed control scheme in Figure 3-4, 3-5. We can see that the actual train speed follows perfectly the referenced speed profile. As the result, the traveled distance also follows the scheduled trajectory, even though it is not the variable under direct control. The power, traction force, acceleration and jerk generally also follow the pattern as in the generating scheme, however with some oscillation at the beginning when the change of speed is high. Especially in the jerk curve, it is indicated that the train jerk continuously oscillates back and forth quite frequently. While it is still inside the constraint range, the performance in terms of passenger comfort might be inferior compared to other control scheme.

It has to be noted that this behavior is dependent on the tuning of the controller. If we choose to design a slower controller, the oscillation in acceleration and jerk can

Figure 3-4: Resulting speed, traveled distance and train power using speed control scheme
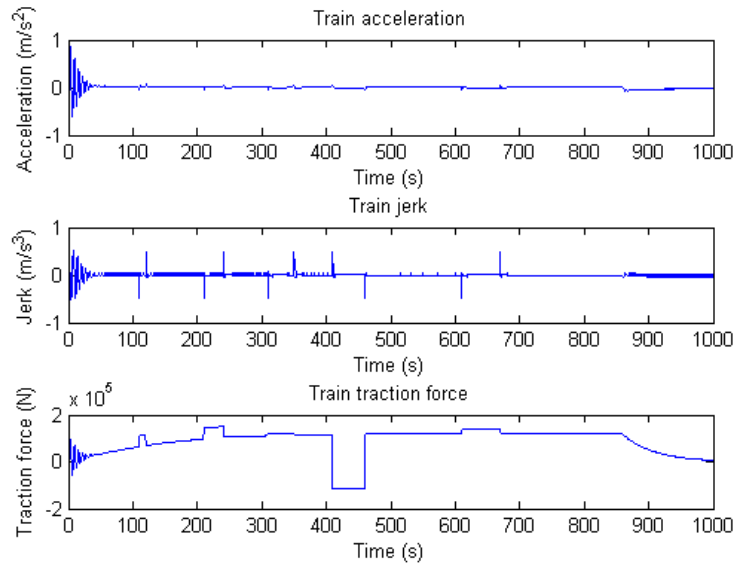
Figure 3-5: Resulting acceleration, jerk and traction/braking force using speed control scheme

be less, but the tracking performance will also be worse. The simulated controller is chosen to have a proper trade off between these two aspects.

Distance cascade control simulation The simulation results for train control using distance cascade scheme is shown in Figure 3-6, 3-7. First of all, the traveled distance also track well the referenced profile. Secondly, even though the speed command only come from the output of the distance controller, the actual speed is also following exactly the generated speed profiles. As in the speed control scheme, we can observe that generally if we are able to control either the train speed or traveled distance, the other quantity will also follow the preset profile to a certain degree.

Looking in other related curves, we can clearly see that this control scheme provides a much smoother performance, with very little oscillation compared to the speed control scheme. The jerk now reaches the limits only a few times during the whole trip. Not only it is more comfortable for the passengers, but also the smoother power and traction force curve suggest a rather stable and less prone to problem operation of the traction motor as well as the traction network.
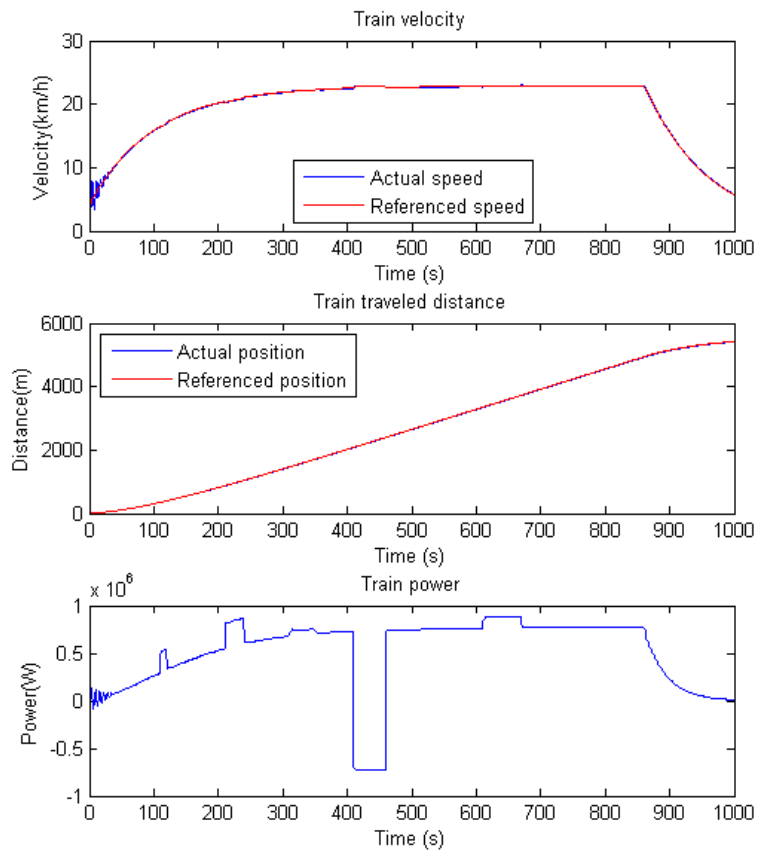
37

Figure 3-6: Resulting speed, traveled distance and train power using distance cascade control scheme
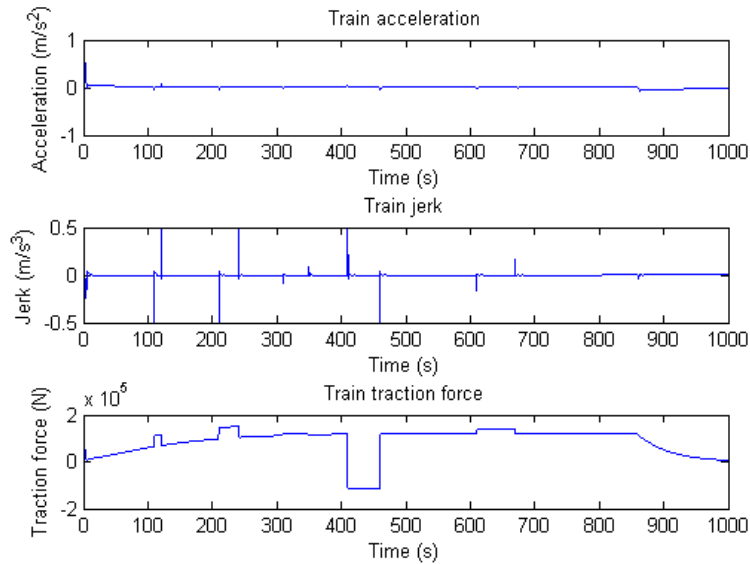
Figure 3-7: Resulting acceleration, jerk and traction/braking force using distance cascade control scheme

Sole distance control simulation   The first impression when we see the resulting graphs for this control scheme (in Figure 3-8, 3-9) is that the tracking performance is not as good under disturbances. During the period between the 400th and 500th second, the train is going down a slope, which makes the actual traveled distance ahead of the reference for a short time before the controller can readjust it. It can also be seen in the speed graph, where the speed rises dramatically during the period and need to be decreased afterwards. Besides, the speed curve also shows some fluctuation at other disturbances presented in the trip such as when the train goes up a slope or goes round a curvy part. Moreover, it is not a matter of controller design, since the simulated one is already chosen to be as fast as possible. The effect is understandable, due to the fact that only traveled distance is controlled. As a result, the power, traction force, acceleration and jerk also experience some oscillation, though not as much as the speed control scheme. However, if the track introduces frequent disturbances, more unwanted fluctuations will appear. With that being said, the ultimate goal of reference tracking is still achieved and it is still a valid control despite the drawbacks.

39

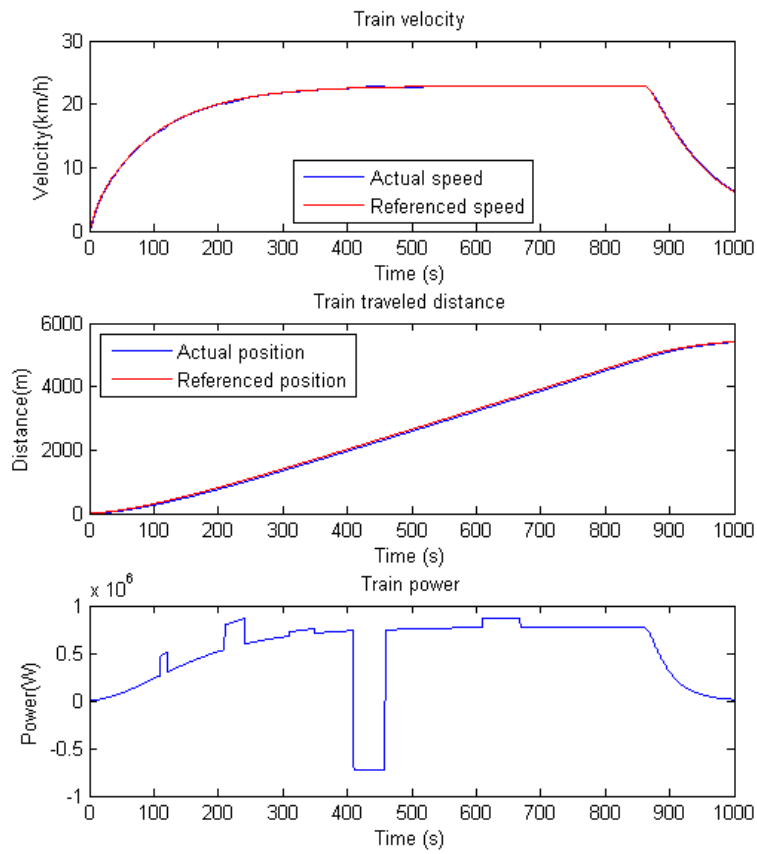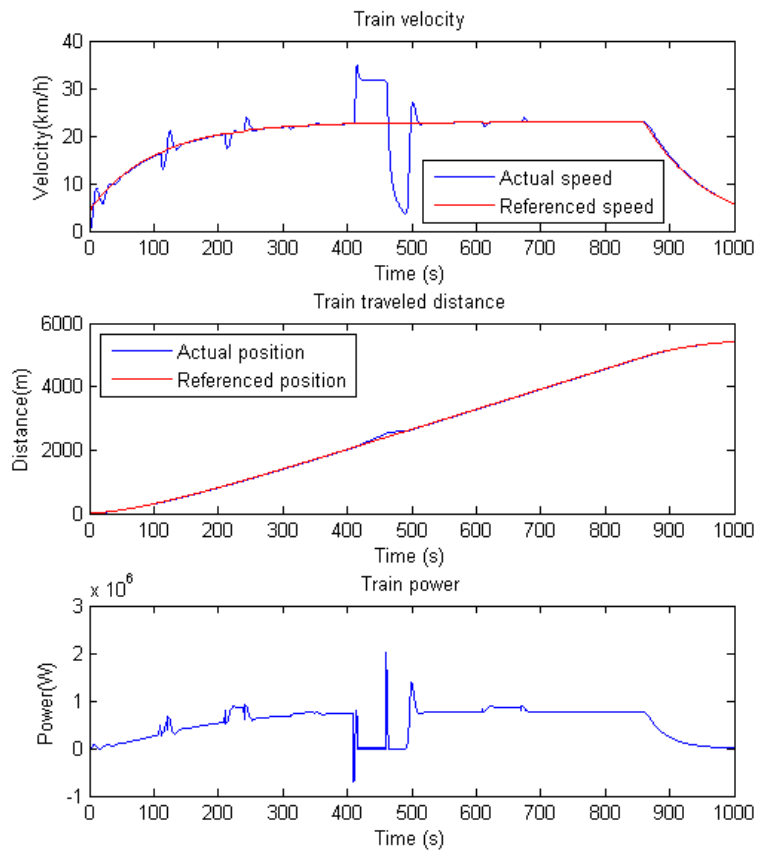Figure 3-8: Resulting speed, traveled distance and train power using sole distance control scheme
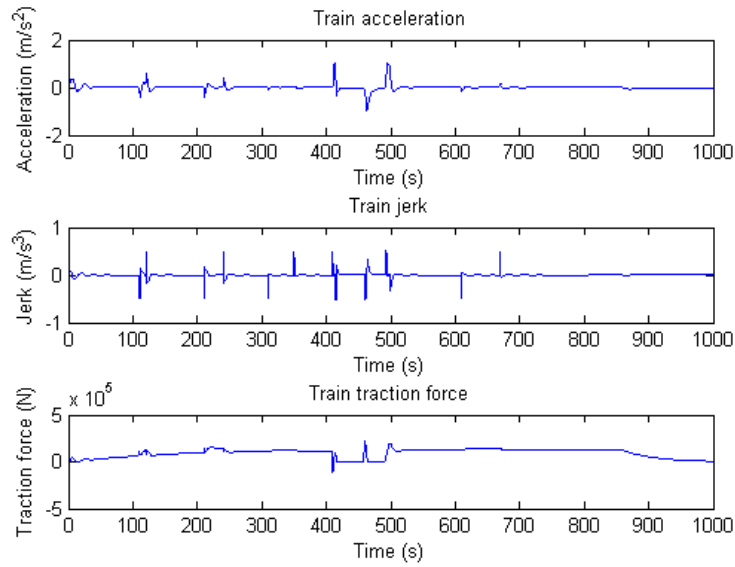
Figure 3-9: Resulting acceleration, jerk and traction/braking force using sole distance control scheme

In conclusion, the distance cascade control yielded the best performance, while the speed control tends to cause fluctuations in jerk and acceleration and the sole distance control react more slowly to disturbances.

On the other hand, to test the robustness of the controllers, we will try to simulate the same train system but with a 1000 tons of train mass. The three resulting sets of graphs are shown in Figure 3-10, 3-11, 3-12. As we can see, heavier train make the all the control less stable and the tracking performance not as good as before. The sole distance control scheme exhibits a complete abnormal speed curve and would require re-tuning of the controller, while the speed control also presents some observable oscillation. Meanwhile, the cascade distance control still results in an acceptable performance, which further solidifies its advantages over the other two schemes.
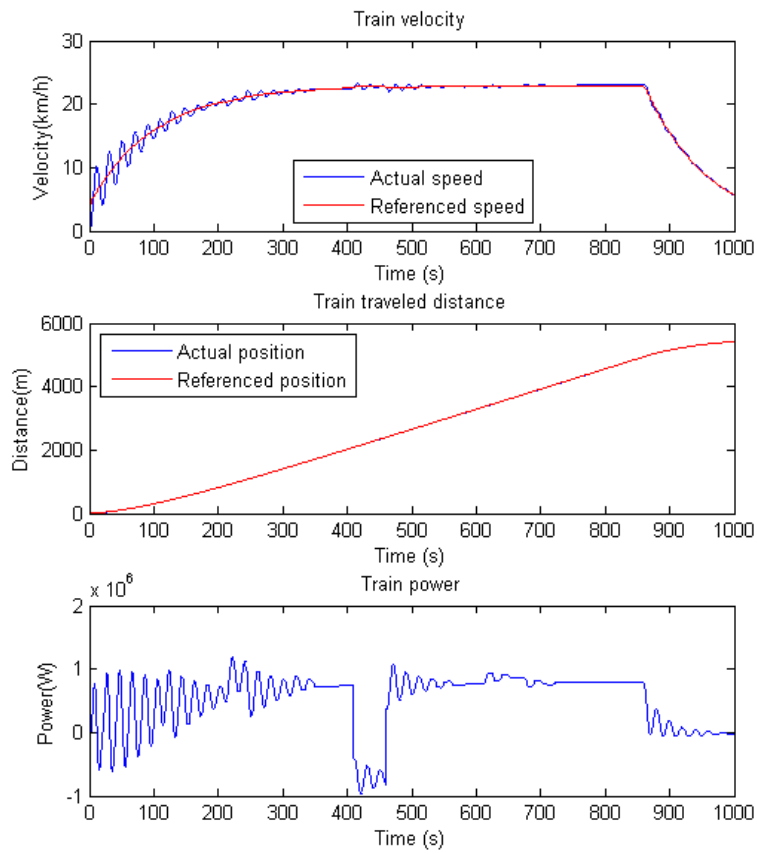
Figure 3-10: Resulting speed, traveled distance and train power using speed control scheme (with 1000-ton train)
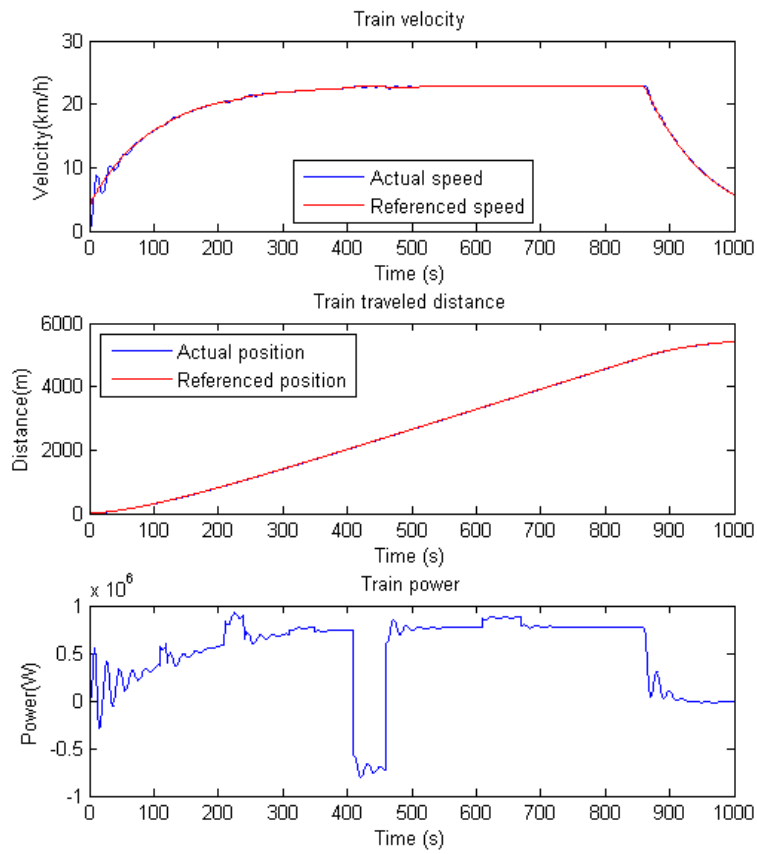
Figure 3-11: Resulting speed, traveled distance and train power using cascade distance control scheme (with 1000-ton train)
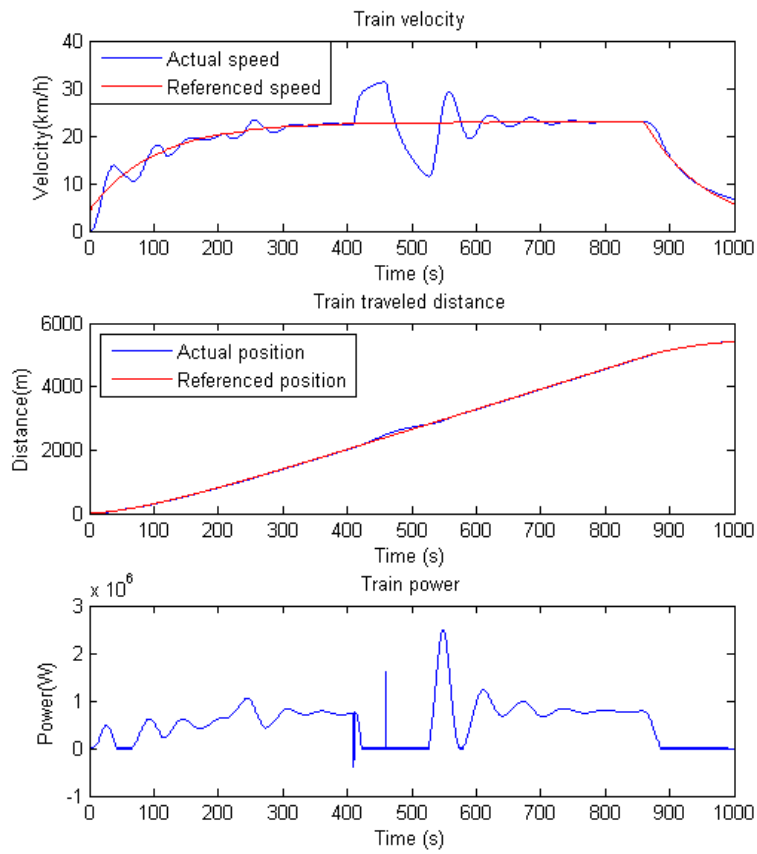
Figure 3-12: Resulting speed, traveled distance and train power using sole distance control scheme (with 1000-ton train)

To observe the effect of power and traction force limitation, we can decrease their limits by 10 times from the previous simulation data, while using the same generated trajectory. Figure 3-13 and 3-14 shows the resulting curves using distance cascade control scheme. From these graphs, we can deduct two observations. First, as mentioned before, the physical limitation of the traction machine will have final say once we get conflicts of limitation. As we can see, since the traction force and the power reach their respected limit, the acceleration goes to more than 2 times the limit, while the jerk even exceeds its limit more than 40 times. Secondly, the limitation of traction force and power have a direct impact in the tracking performance of the control. Since the train lack the power/force to propel it to reference speed and distance, deviations unavoidably appear. In this case, it is deliberately set by us to have this effect and usually the trajectory is set up take into account the train's traction machine capacity and the track condition. However, in reality this can also happen with the presence of line saturation or over current protection.
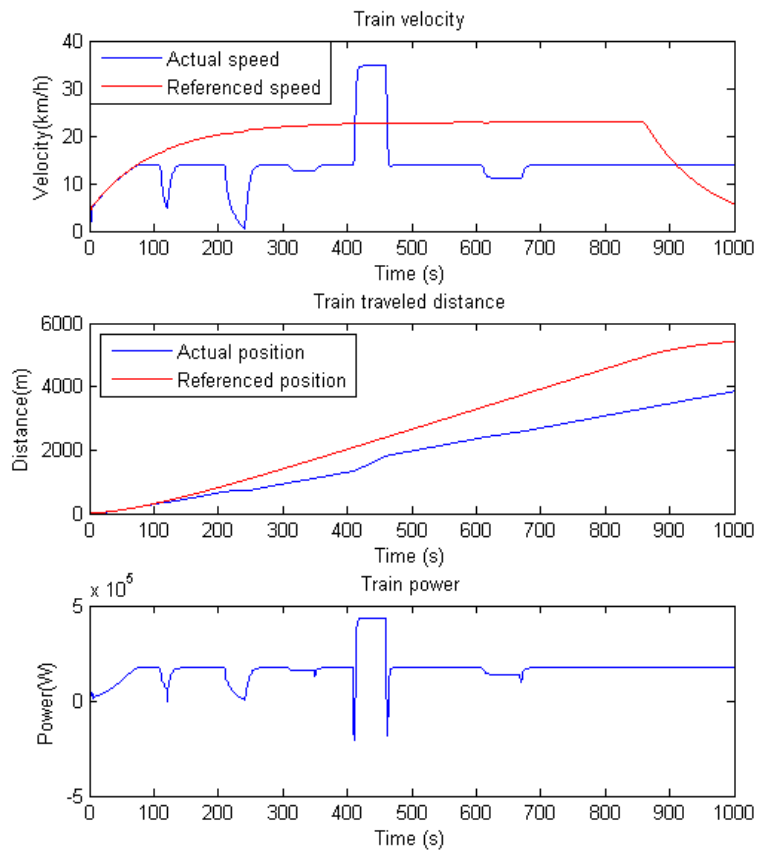
Figure 3-13: Resulting speed, traveled distance and train power using cascade distance control scheme with traction machine capacity of 10 times less
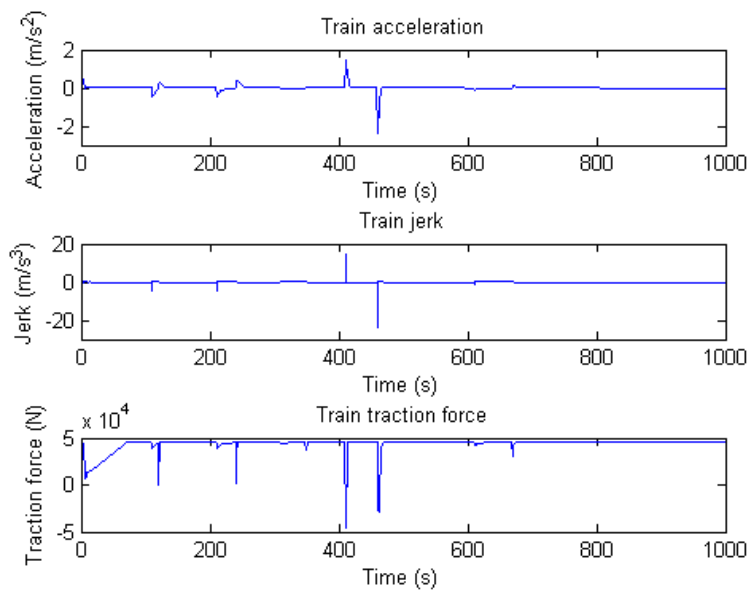
Figure 3-14: Resulting speed, traveled distance and train power using cascade distance control scheme with traction machine capacity of 10 times less

Chapter 4

Integration with electric simulator

As mentioned before, one important goal of simulating the motion of the train is to integrate it to the electric simulator to have the power flow of the network solved. The electric modeling and simulator was done in a separate work, only critical notes about it will be listed out here.

4.1   Electric simulator overview

First of all, it is needed to have a grasp of the railway traction network. In the world, both DC and AC traction networks are utilized. AC traction networks are the standard in Germany, Austria, Norway, Sweden, etc. Meanwhile, the DC alternative are more popular in countries like Spain, Italy, France. Within each countries, there can also be lines that run on DC system and others that run on AC system. Generally, the traction network can be represented in Figure 4-1, where we have a normal electricity generation, transmission and distribution network which feeds to AC substations and DC substations under management of railway operators and propel the trains.

In this simulation, we will focus on the DC traction network, which is the standard in Spanish railway system. The main scheme is shown in Figure 4-2, in which we have the AC system, the AC/DC conversion (Link) system and the DC system which feeds to the trains.

The train is generally considered a load, but it can also inject power to the grid.
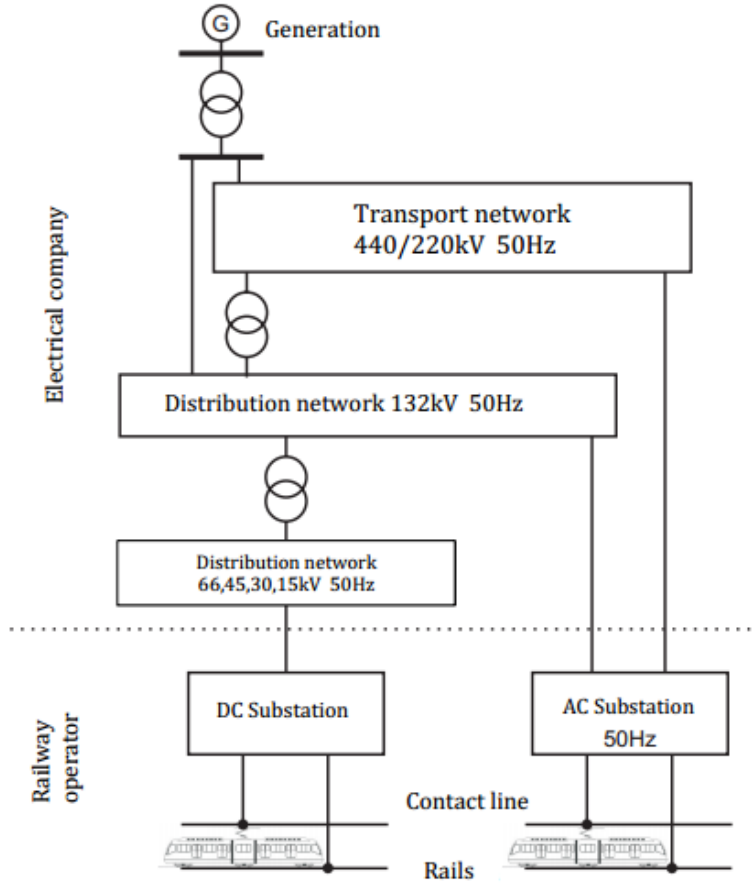
Figure 4-1: General configuration of traction networks in the world [39].

More importantly, the train changes position as a function of time, which also leads to a change in system topology. Therefore, stating the new problem after each instant of time is not possible and we have to find a way to describe the problem more systematically. In order to do so, we will use graph theory to characterize the problem. The vertices in the graph are the AC substation and nodes, the link nodes, the DC substation and birfucation point, and the trains themselves. With some assumptions that allows the number of nodes and their enumeration is unchanged in all instants, we can then formulate and solve the power flow problem with non linear modeling and optimization equations. The node enumeration criteria is in the order of trains - DC nodes - Link nodes - AC nodes. One important feature of a graph is that it has matrix representations. For a simple digraph (one whose edges are formed by ordered pair of nodes and there is no self loop), an adjacency matrix with the dimension (n,n)
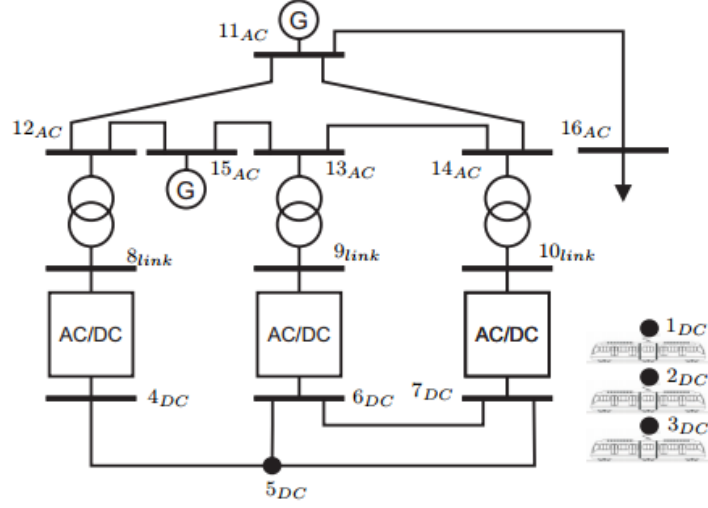
Figure 4-2: Topology of the simulated electric traction network [39].

where n is the number of nodes can be defined as:

$$
\Lambda_{i,j} = \begin{cases} 1, \ (\exists \ adjacency \ between \ i \ and \ j) \wedge (i > i) \\ 0, \ other \ cases \end{cases} \tag{4.1}
$$

Besides, an incident matrix (k,n) can also be used to represent the graph with n nodes and k edges:

$$
\Gamma_{i,j} = \begin{cases} 1, \ the \ tail \ of \ edge \ i \ is \ node \ j \\ -1, \ the \ head \ of \ edge \ i \ is \ node \ j \\ 0, \ other \ cases \end{cases} \tag{4.2}
$$

Applying to this case, we can have the adjacency matrix for the whole network as shown in Figure 4-3. It comprises of sub-matrices from DC, Link and AC sub-graphs, where:

n_t is the number of train nodes

$n_S^D C$ is the number of DC nodes

n_N^L is the number of link nodes

$n_S^A C$ is the number of AC nodes

$n_N^D C$ is the number of DC subsystems including train nodes

51

n_N^AC is the number of AC subsystems including link nodes
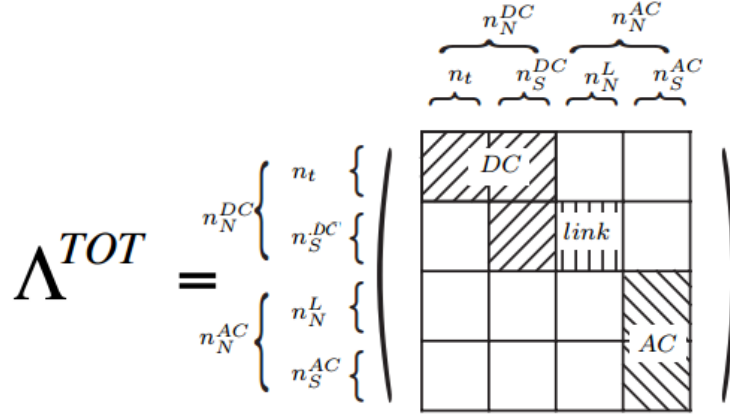
Figure 4-3: Adjacency matrix of the whole network [39].

For the edge enumeration, we also starts from DC subsystems to link subsystems and AC subsystems. Starting from node 1, we enumerate all out going edges based on ascending order of the tail node before moving to node 2 and so on. That way, we can obtain the incident matrix by going through the adjacency matrix, knowing that each not-null element represent an edge. One important note to overcome the change in topology of the system is that we always consider all possible connections between nodes in all instants. That way, we avoid the appearance and disappearance of some edges as the result of moving loads. As the result of the enumeration criteria, we have a complete edge list in table 4.1

For the formulation, we use ordinary equations such as Kirchhoff's laws and link them up with the incident matrices to form a set of equations needed to solve the power flow problem. For AC lines model, using dq synchronous reference frame transformation, we have the following familiar equation:

$$
\begin{cases}
v_d = Ri_d - \omega Li_q \\
v_q = Ri_q + \omega Li_d
\end{cases}
\tag{4.3}
$$

Table 4.1: Edge enumeration

Subsystem	Terminals	Edge
DC	(1,2)	1
DC	(1,3)	2
DC	(1,4)	3
DC	(1,5)	4
DC	(1,6)	5
DC	(1,7)	6
DC	(2,3)	7
DC	(2,4)	8
DC	(2,5)	9
DC	(2,6)	10
DC	(2,7)	11
DC	(3,4)	12
DC	(3,5)	13
DC	(3,6)	14
DC	(3,7)	15
DC	(4,5)	16
DC	(5,6)	17
DC	(5,7)	18
DC	(6,7)	19
Link	(4,8)	20
Link	(6,9)	21
Link	(7,10)	22
AC	(8,12)	23
AC	(9,13)	24
AC	(10,14)	25
AC	(11,12)	26
AC	(11,14)	27
AC	(11,16)	28
AC	(12,15)	29
AC	(13,14)	30
AC	(13,15)	31

which can be re-written in the form of:

$$
\begin{pmatrix} v_d \\ v_q \end{pmatrix} = \begin{pmatrix} R & -\omega L \\ \omega L & R \end{pmatrix} \cdot \begin{pmatrix} i_d \\ i_q \end{pmatrix}
\tag{4.4}
$$

where

v_d is d axis voltage

i_d is d axis current

v_q is q axis voltage

i_q is q axis current

R is the line resistance

L is the line inductance

ω is the grid frequency

For example, applying Kirchoff's voltage law (KVL) to edge 23 (between node 8 and node 12) we have:

$$
\begin{pmatrix} v_{8d} - v_{12d} \\ v_{8q} - v_{12q} \end{pmatrix} = \begin{pmatrix} R_{23} & -\omega L_{23} \\ \omega L_{23} & R_{23} \end{pmatrix} \cdot \begin{pmatrix} i_{23d} \\ i_{23q} \end{pmatrix}
\tag{4.5}
$$

Similarly, we can write KVL euquations in synchronous reference frame for all the AC edges, which can be generalized in the form:

$$
\Gamma^{AC}(\mathbf{v}_{Nd}^{AC})^T = \mathbf{R}_E^{AC}(\mathbf{i}_{Ed}^{AC})^T - \mathbf{X}_E^{AC}(\mathbf{i}_{Eq}^{AC})^T
\tag{4.6}
$$

$$
\Gamma^{AC}(\mathbf{v}_{Nq}^{AC})^T = \mathbf{X}_E^{AC}(\mathbf{i}_{Ed}^{AC})^T + \mathbf{R}_E^{AC}(\mathbf{i}_{Eq}^{AC})^T
\tag{4.7}
$$

where

Γ^{AC} is the incident matrix of AC subsystem (considering all edges possible)

$\mathbf{v}_{Nd}^{AC}$ is the array of d axis node voltages

$\mathbf{v}_{Nq}^{AC}$ is the array of q axis node voltages

$\mathbf{i}_{Ed}^{AC}$ is the array of d axis edge current

$\mathbf{i}_{Eq}^{AC}$ is the array of q axis edge current

$$\mathbf{R}_E^{AC} = \begin{pmatrix} \mathbf{R}_E^{transf} & 0 \\ 0 & \mathbf{R}_E^{lineAC} \end{pmatrix} \text{ with } \mathbf{R}_E^{transf} \text{ being the array of transformer edges'}$$

resistance and $\mathbf{R}_E^{lineAC}$ being the array of AC line resistance

$$\mathbf{X}_E^{AC} = \begin{pmatrix} \mathbf{X}_E^{transf} & 0 \\ 0 & \mathbf{X}_E^{lineAC} \end{pmatrix} \text{ with } \mathbf{X}_E^{transf} \text{ being the array of transformer edges'}$$

reactance and $\mathbf{X}_E^{lineAC}$ being the array of AC line reactance
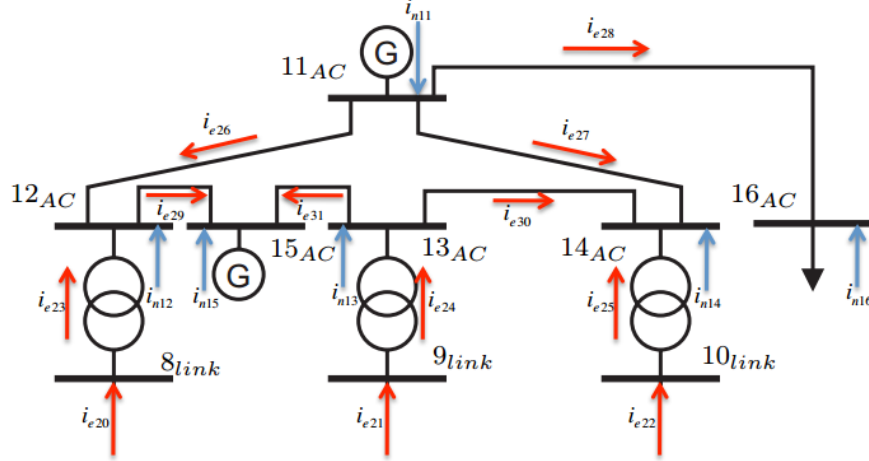
Figure 4-4: AC subsystem diagram

Using Kirchoff's current laws (KCL) on the nodes, we will form another set of equations regarding the currents.

For link node 8, we have:

$$\begin{pmatrix} 0 \\ 0 \end{pmatrix} = \begin{pmatrix} -i_{e20d} + i_{e23d} \\ -i_{e20q} + i_{e23q} \end{pmatrix} \tag{4.8}$$

For AC node 12, we have:

$$\begin{pmatrix} i_{n12d} \\ i_{n12q} \end{pmatrix} = \begin{pmatrix} -i_{e23d} - i_{e26d} + i_{e29d} \\ -i_{e23q} - i_{e26q} + i_{e29q} \end{pmatrix} \tag{4.9}$$

Similarly with other link nodes and AC nodes, we can generalized these KCL equations into the form:

$$(\Gamma^{AC})^T (\mathbf{i}_{Ed}^{AC})^T = \mathbf{I}.[\mathbf{i}_{Ed}^L \ \mathbf{i}_{Nd}^{AC}]^T \tag{4.10}$$

$$(\Gamma^{AC})^T(\mathbf{i}_{Eq}^{AC})^T = \mathbf{I}.[\mathbf{i}_{Eq}^L \ \mathbf{i}_{Nq}^{AC}]^T \tag{4.11}$$

where

$\mathbf{I}$ is the unit (n,n) matrix with n being the number of AC edges

$\mathbf{i}_{Ed}^L$ is the array of d axis link edge current

$\mathbf{i}_{Eq}^L$ is the array of q axis link edge current

$\mathbf{i}_{Nd}^{AC}$ is the array of d axis AC node current

$\mathbf{i}_{Nq}^{AC}$ is the array of q axis AC node current

others are defined as in KVL euquations.
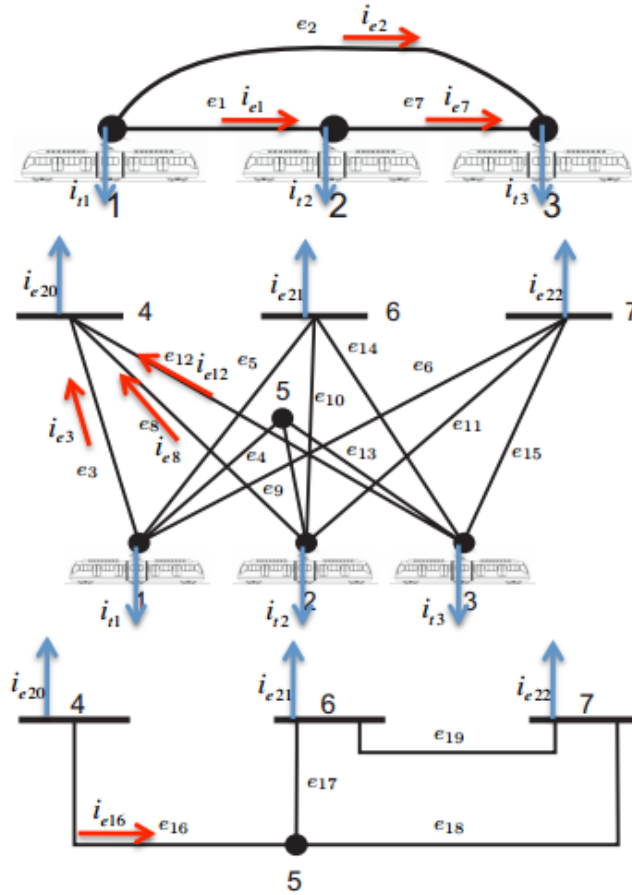
Figure 4-5: DC subsystem diagram [39]

Similarly, we can derive all equations needed to solve the DC subsystems whose diagram is shown in Figure 4-5. Since it is not the purpose of this thesis to elaborate the electric solver formulation procedure, we will only list out main equations here.

$$(\Gamma^{DC})^T(\mathbf{v}_N^{DC})^T = \mathbf{R}_E^{DC}(\mathbf{i}_E^{DC})^T \tag{4.12}$$

where

Γ^{DC} is the incident matrix of DC subsystem (considering all possible edges)

$\mathbf{v}_N^{DC}$ is the array of DC subsystem nodes' voltages

$\mathbf{i}_E^{DC}$ is the array of DC subsystem edges' currents

$\mathbf{R}_E^{DC} = \begin{pmatrix} \mathbf{R}_E^t & 0 \\ 0 & \mathbf{R}_E^{lineDC} \end{pmatrix}$ with $\mathbf{R}_E^t$ being the array of train edges' resistance and

$\mathbf{R}_E^{lineDC}$ being the array of DC line resistance

$$(\Gamma^{AC})^T(\mathbf{i}_E^{DC})^T = \mathbf{S}.[\mathbf{i}_t^{DC} \ \mathbf{i}_E^L] \tag{4.13}$$

where

$\mathbf{i}_t^{DC}$ is the array of train's current

$\mathbf{i}_E^L$ is the array of edges current connected from DC lines to link nodes.

$\mathbf{S} = \begin{pmatrix} \mathbf{I} & 0 \\ 0 & \mathbf{S}^L \end{pmatrix}$ with $s_{ii}^L = 1$ if the DC node i is connected to AC subsystem through

a link node and $s_{ii}^L = 0$ if the DC node i is not connected to AC subsystem through

a link node.

Others are defined as previously in AC subsystem equations.

For AC buses, slack, PQ, PV buses introduce different set of equations:

$$For \ PQ \ bus: \begin{cases} P_i = v_{nid}.i_{nid} + v_{niq}.i_{niq} \\ Q_i = v_{niq}.i_{nid} - v_{nid}.i_{niq} \end{cases} \tag{4.14}$$

$$For \ PV \ bus: \begin{cases} P_i = v_{nid}.i_{nid} + v_{niq}.i_{niq} \\ |v_{ni}| = \sqrt{v_{nid}^2 + v_{niq}^2} \end{cases} \tag{4.15}$$

$$For \ slack \ bus: \begin{cases} v_{nid} = v_i^{specified} \\ v_{niq} = 0 \end{cases} \tag{4.16}$$

where

v_{nid} is the d axis node voltage

v_{niq} is the q axis node voltage

i_{nid} is the d axis node current

i_{niq} is the q axis node current

P_i is the active power

Q_i is the reactive power

For train nodes, we take into account a squeeze control. When the train brakes, if the catenary voltage is increased over a given number, the power will be linearly diminished until the maximum voltage is reached. Above this maximum voltage, the system will not get any regenerated power.

$$For\ traction\ process : i_{ti} = \frac{P_i}{v_{ni}} \tag{4.17}$$

$$For\ braking\ process : i_{ti} = \begin{cases} \frac{P_i}{v_{ni}} \ if \ v_{ni} \leq V_c \\ m(v_{ni} - V_{max}) \ if \ V_c < v_{ni} \leq V_{max} \\ 0 \ if v_{ni} > V_{max} \end{cases} \tag{4.18}$$

with $m = \frac{I_0}{V_{max} - V_0}$

V_0, V_c, V_{max} are the critical points described in figure 4-6.

i_{ti} is the train current

v_{ni} is the train node voltage

For each link nodes, we have three more equations simply based on power conservation and Ohm's law as following:

$$\mathbf{v}^{AC}_{Ndj}.\mathbf{i}^{L}_{Edk} + \mathbf{v}^{AC}_{Nqj}.\mathbf{i}^{L}_{Eqk} - \mathbf{v}^{DC}_{Ni}.\mathbf{i}^{L}_{Ek} = 0 \tag{4.19}$$

$$\mathbf{v}^{AC}_{Nqj}.\mathbf{i}^{L}_{Edk} - \mathbf{v}^{AC}_{Ndj}.\mathbf{i}^{L}_{Eqk} = 0 \tag{4.20}$$
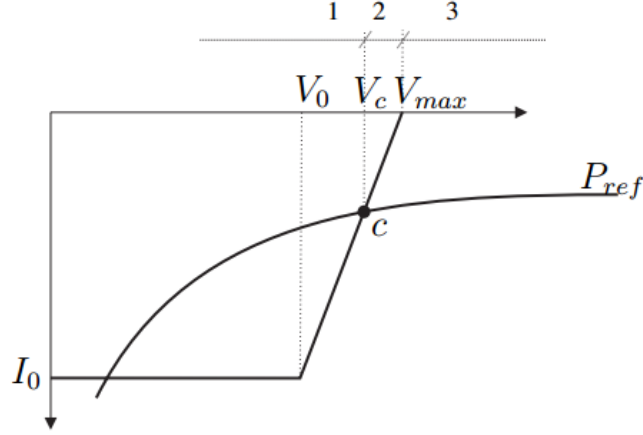
Figure 4-6: Braking squeeze control diagram

$$\begin{cases} \mathbf{i}_{Ek}^L = \frac{1}{R_{eq}}(\mathbf{v}_{Ni}^{DC} - \sqrt{(\mathbf{v}_{Ndj}^{AC})^2 + (\mathbf{v}_{Nqj}^{AC})^2}) \; if \; v_{Ni}^{DC} \leq v_{Nj}^{AC} \\ \mathbf{i}_{Ek}^L = 0 \; if \; v_{Ni}^{DC} > v_{Nj}^{AC} \end{cases} \qquad (4.21)$$

where

$\mathbf{v}_{Ndj}^{AC}$ is the d axis AC side node voltage

$\mathbf{v}_{Nqj}^{AC}$ is the q axis AC side node voltage

$\mathbf{v}_{Ni}^{DC}$ is the DC side node voltage

$\mathbf{i}_{Edk}^L$ is the d axis AC side current

$\mathbf{i}_{Eqk}^L$ is the q axis AC side current

$\mathbf{i}_{Ek}^L$ is the DC side current

R_{eq} is the equivalent resistance of the rectifier

Above is only a quick glance into the equations derived from the electric model. Details of graph theory, how to apply it to the railway traction network and the problem formulation procedure as well as the non linear solver can be seen in [39].
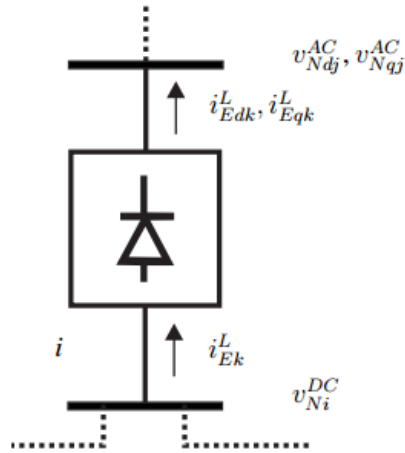
Figure 4-7: Link node model

4.2 Linking up with train simulator

What we will do in this part is to use the simulation results in previous part, in particular the train position and the consumed/injected power, as the input to the electric simulator. These variables, in Matlab platform, will be passed to the electric solver in the cell array form, each one represent one instant and each instant will be solved separately. In this simulation, we will suppose the train will go from node 5 to node 7, the distance from these two nodes is set to be 10km. The other two trains in the existing system will be kept idle in terms of both position and power, assumed to be fixed loads for simplicity. Note that all the assumptions we have made in this thesis do not make the simulation lose its generality. One can easily change the data at will to produce other simulations.

As the result, the electric simulator was able to solve the power flow problem for each and every instant with the input data from train simulation. In this simulation, the electric simulator is programmed to solve the power flow at 1Hz, or in other words we pass the data every 10 samples of the train simulator to the electric solver. In practice, these frequencies depends on the existing facility and computers of the system. The code block that is responsible for this coupling function between train simulator and electric simulator is written in a separate script and can be run after any

60

train simulation, whether it is distance cascade control, sole distance control or speed control. The final results are then stored in a solution.mat file, which includes power flow results at AC/DC substations, link nodes, train nodes, AC/DC/Link lines. One example of a complete result solved for the 500th second instant of train simulation using distance cascade control can be shown as following figures (note that the 3rd train is the actual simulated train):

'Num'	'P_ref(W)'	'P_act(W)'	'V_cat(V)'	'I(A)'
1	443000	4.4300e+05	1.4187e+03	312.2581
2	380000	3.8000e+05	1.3710e+03	277.1762
3	1.3941e+06	1.3941e+06	1.3526e+03	1.0307e+03

Figure 4-8: Train node result at 500th second instant (distance cascade control scheme).

'Num'	'P(W)'	'V_Sub(V)'	'I(A)'
4	-9.2550e+05	1.5904e+03	-581.9473
5	1.1671e-12	1.3719e+03	8.5073e-16
6	-5.0332e+05	1.6242e+03	-309.8825
7	-1.1417e+06	1.5676e+03	-728.2725

Figure 4-9: DC substation node result at 500th second instant (distance cascade control scheme).

'Num'	'P(W)'	'Q(Var)'	'V_lnk(V)'	'III(A)'
8	9.2550e+05	-0.0580	1.2298e+03	434.5069
9	5.0332e+05	-0.0389	1.2305e+03	236.1634
10	1.1417e+06	-0.0837	1.2260e+03	537.6153

Figure 4-10: Link node result at 500th second instant (distance cascade control scheme).

We can also compare the resulting voltages and currents of the train node, using three proposed control schemes. As we can see in Figure 4-15, 4-16, 4-17, there are significant differences between the behavior of the sole distance control with the other two control schemes. This behavior was also reflected in the train simulation result earlier, where speed control and distance cascade control had nearly the same curves (with just a little oscillation in speed control) while sole distance control gave

'Num'	'P(W)'	'Q(Var)'	'V_Sub(V)'	'|I|(A)'
11	-4.0662e+06	-1.2975e+06	2.5000e+04	98.5694
12	1.2672e-11	-8.4700e-11	2.4359e+04	2.0299e-15
13	8.0753e-12	8.0741e-12	2.4283e+04	2.7150e-16
14	3.0216e-11	-5.4782e-11	2.4335e+04	1.4843e-15
15	4.0000e+05	-0.0019	2.4303e+04	9.5024
16	1.0000e+06	8.0000e+05	2.3561e+04	31.3809

Figure 4-11: AC substation node result at 500th second instant (distance cascade control scheme).

'Num'	'from(node)'	'to(node)'	'I(A)'
1	1	2	269.6572
2	1	3	0.0049
3	1	4	-581.8976
4	1	5	0.0034
5	1	6	-0.0151
6	1	7	-0.0110
7	2	3	0.0013
8	2	4	-0.0161
9	2	5	-7.4711
10	2	6	-0.0186
11	2	7	-0.0145
12	3	4	-0.0175
13	3	5	-206.4468
14	3	6	-0.0200
15	3	7	-824.1775
16	4	5	0.0161
17	5	6	-213.8840
18	5	7	-0.0144
19	6	7	95.9448

Figure 4-12: DC line result at 500th second instant (distance cascade control scheme).

'Num'	'from(node)'	'to(node)'	'|I|(A)'
23	8	12	22.1055
24	9	13	12.0148
25	10	14	27.3512
26	11	12	36.1664
27	11	14	34.8023
28	11	16	31.3809
29	12	15	14.0610
30	13	14	7.4563
31	13	15	4.5657

Figure 4-13: AC line result at 500th second instant (distance cascade control scheme).

'Num'	'from(node)'	'to(node)'	'|I_AC|(A)'	'I_DC(A)'
20	4	8	434.5069	-581.9473
21	6	9	236.1634	-309.8825
22	7	10	537.6153	-728.2725

Figure 4-14: Link line result at 500th second instant (distance cascade control scheme).

more abnormal results. Especially when we look at the train current, while the speed control and distance cascade control yield similar and stable curves between 500A and -500A, the train in sole distance control requires a current peak around 1000A in several occasions. In practice, when over current protection is implemented, this can trigger the protection and subsequently lead to deviation in the train power. As the result, deviation in train traveled distance appears and eventually make the control oscillate even more and/or the goal of schedule control will not be achieved. That couples with the abrupt changes in both voltage and current curves make the sole distance control strategy less favorable, and even more so if the track presents more disturbances.

Again, we will try a simulation in which the train now having 1000 tons of mass. The train node voltage and current curves in each control scheme are shown in Figure 4-18, 4-19, 4-20. Although appeared to be smoother (due to the its slow reaction nature), the sole distance control still present a significantly higher current peak (around 1800A) compared to the other two schemes.

Figure 4-15: Train node voltage and current (speed control scheme).

Figure 4-16: Train node voltage and current (distance cascade control scheme).
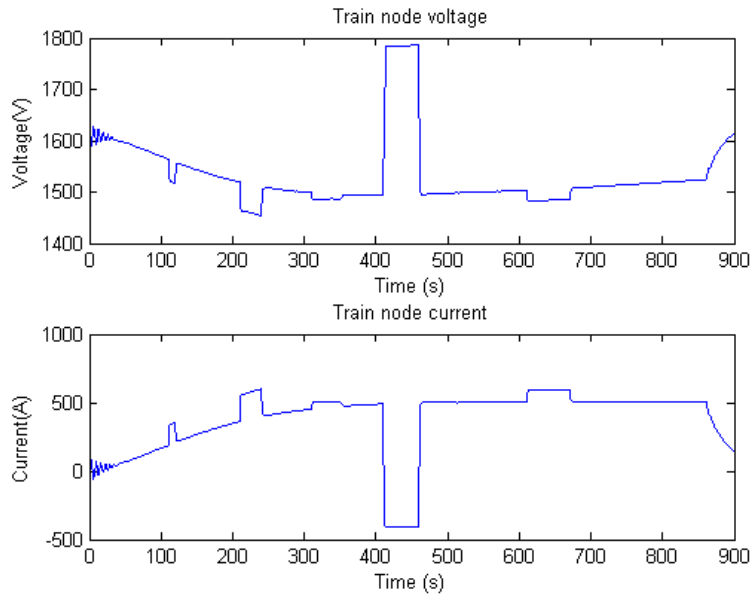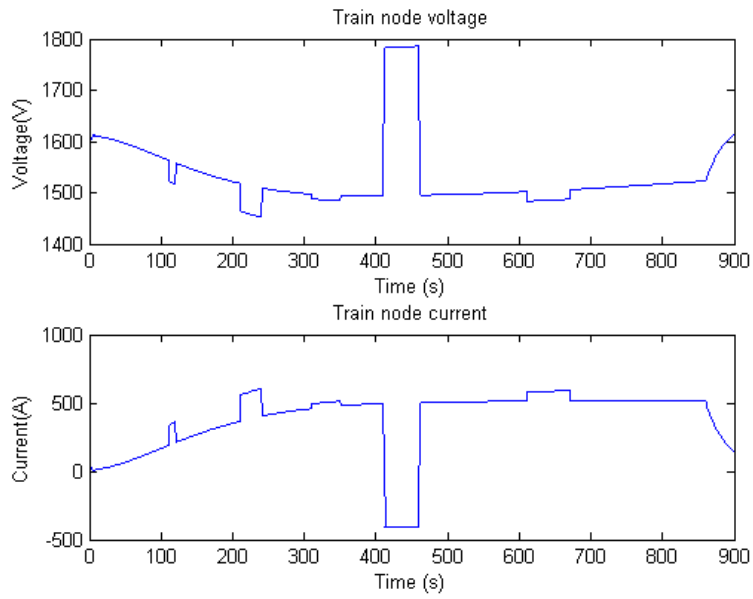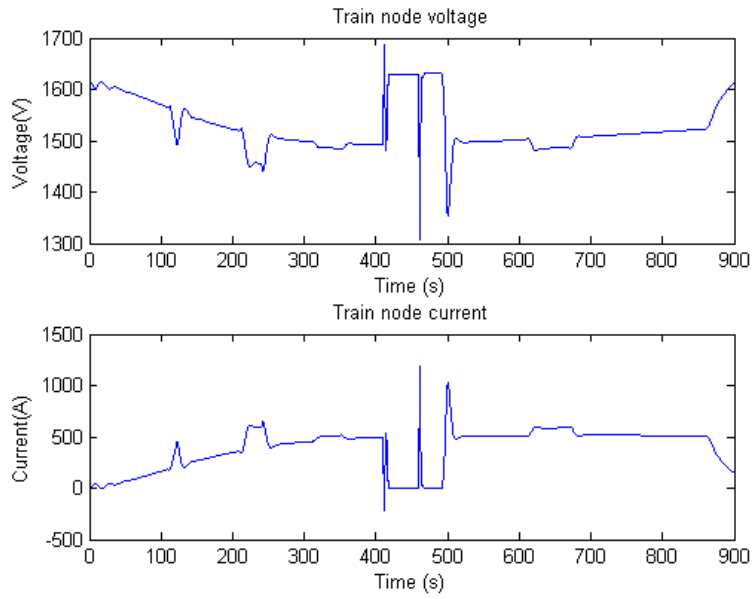
Figure 4-17: Train node voltage and current (sole distance control scheme).
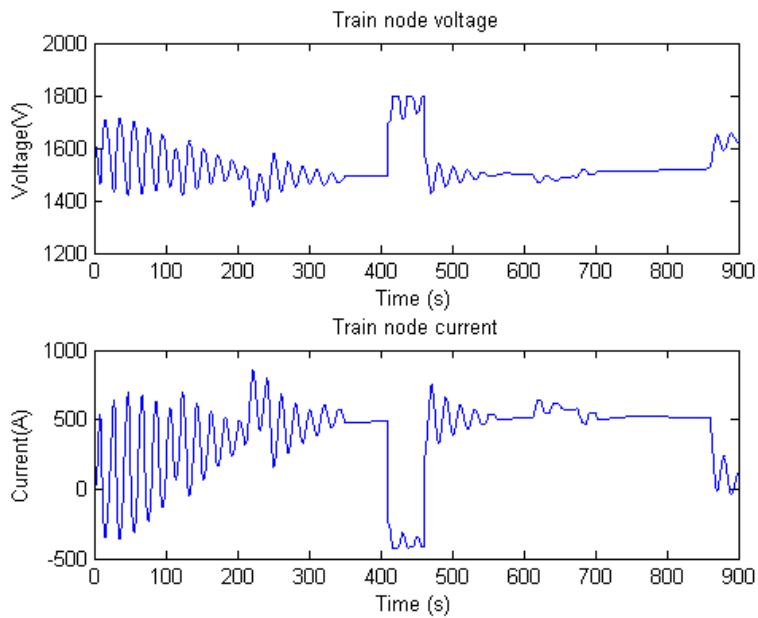
Figure 4-18: Train node voltage and current (speed control scheme with 1000-ton train).
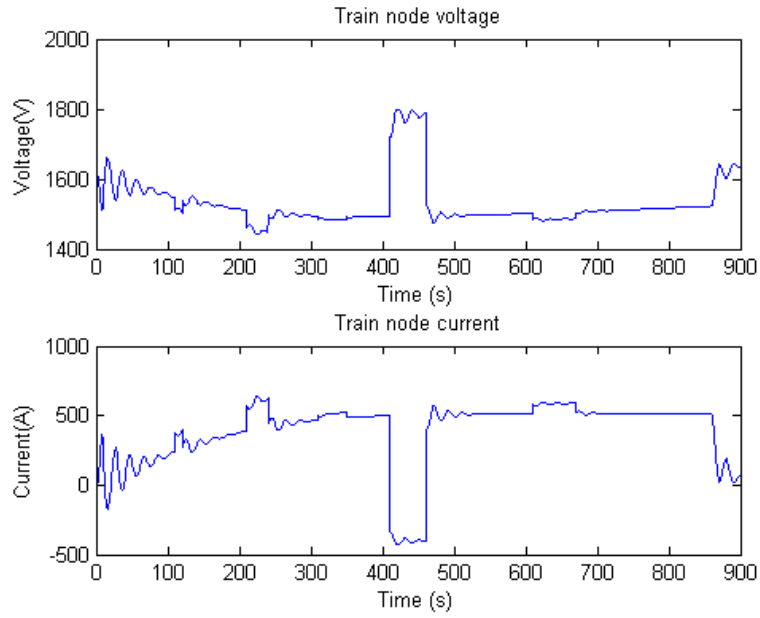
Figure 4-19: Train node voltage and current (distance cascade control scheme with 1000-ton train).
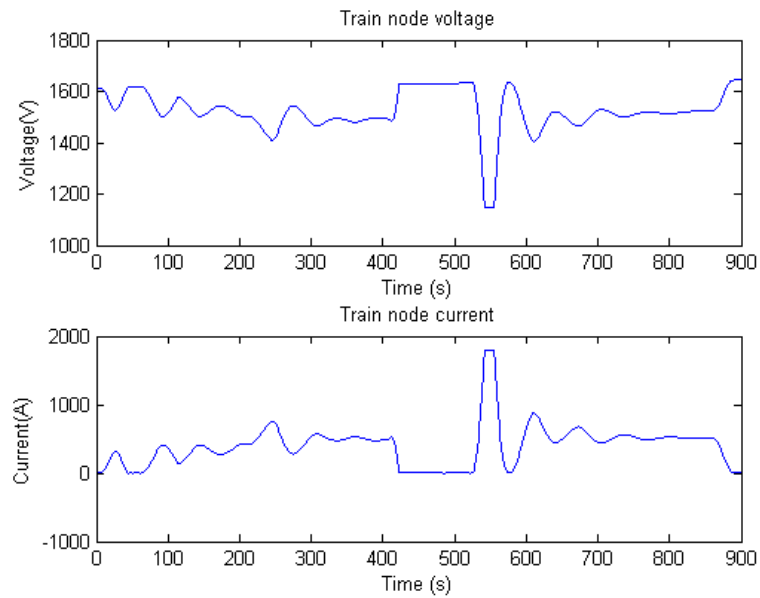
Figure 4-20: Train node voltage and current (sole distance control scheme with 1000-ton train).

We can have a further look into the network, with DC line connecting from DC node 7 to the train in Figure 4-21. The same can be observed here that the sole distance control yields a substantially higher current peak on the line. The generated power from the slack bus is shown in Figure 4-22. Even though it's a relatively far node from the train, its excessive 1MW peak that had to be generated more in the sole control scheme suggests that the control strategy of a train can have a great effect to the whole system network. That solidifies even more the need of coupling train simulator and electric simulator to present a complete problem and have the base for further optimization implemented on either train control algorithm or traction network configuration.
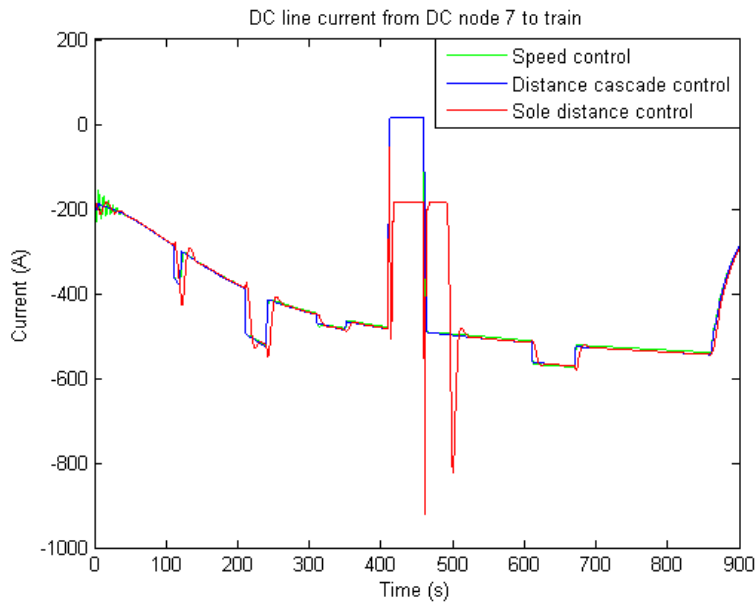
Figure 4-21: DC line current from node 7 to train.
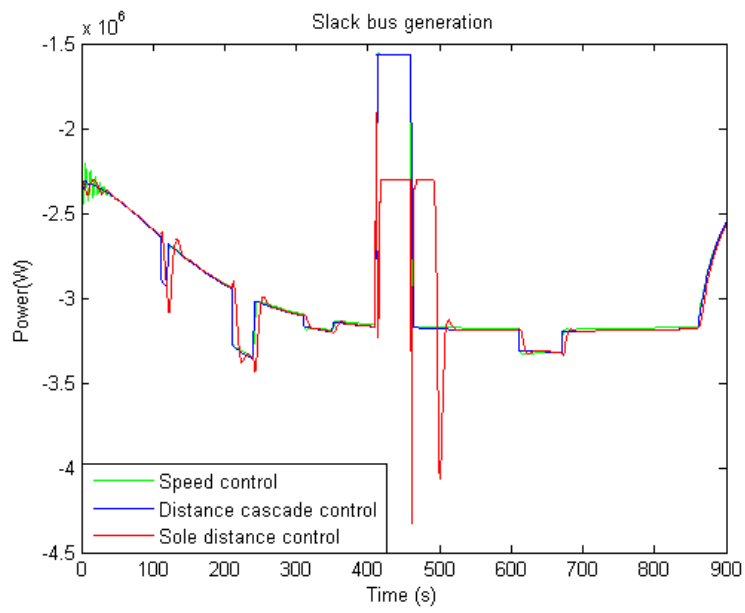
Figure 4-22: Slack bus generation level.

Chapter 5

Conclusion and future development

The thesis focuses on the characterization of train motion by using a point mass model and several control schemes including speed control, distance cascade and sole loop controls. One random and simple speed and position profile is generated and used as the reference for the three control schemes, whose controllers are based on Proportional - Integral form. The system is then simulated on Matlab script platform with typical train data. All three control schemes are proved to work well in terms of reference tracking and eventually the goal of matching the trip's schedule. However, in terms of stable performance taking into account other factors such as acceleration, jerk, power and traction/braking force, the distance cascade control prevails over the other two. Though not necessarily using state of the art schedule control and speed profile optimization technique in literature, the control schemes are sufficient to simulate the kinematic of the train under the action of either the train operator or the ATO system. The resulting variables, position and power in particular, is then used to link up with the electric simulator, which solve the power flow of the traction network. The process works properly and the electric simulator is able to solve the network under changes in the moving load (which is the train) through out the whole train journey.

For future development, the topic of train control can be further enhanced by applying the optimization approach when creating the trajectory as well as using a more advanced schedule control technique. Possible ways existing in literature were

mentioned in the introduction part. Regarding the integration of train simulator and electric simulator, we can further eliminate the decoupling nature between these two systems by simulating their real time interaction. For example, when additional components of the train system such as over current protection or catenary voltage constraint is implemented, the real power consumed or injected might be different than the one calculated by train simulator. In such situation, the train control system have to adapt to real time deviations of controlled and influencing variables to keep a proper reference tracking performance. Besides, a number of trains can also be added in the system, giving additional constraints regarding the power flow solution as well as the time table among trains. By adding and perfecting these aspects, the whole railways traction networks can be simulated and be the base for further improvement ideas.

Appendix A

Simulation data for electric simulator

In this appendix, the data used for simulation of the electric traction network. As described in chapter 4, the topology under consideration has 3 train nodes, 4 DC substations and bifurcation point, 3 link nodes, 6 AC substations and AC bus. The full data for the nodes and the lines are elaborated here in the following tables:

Table A.1: General parameters

Parameter	Value
Base power S_b	2MW
Base voltage primary side V_{1b}	24kV
Base voltage secondary side V_{2b}	1221V
Base voltage DC side V_{db}	1648.93V
Short circuit power in substation S_{cc}	500MW
Rated frequency f_b	50Hz

where

S_b is base power

V_{1b} is base voltage primary side

V_{2b} is base voltage secondary side

V_{db} is base voltage DC side

S_{cc} is short circuit power in substation

f_b is rated frequency

Other base parameters can be calculated as following:

Base current in AC subsystem:

$$I_{b1} = \frac{S_b}{\sqrt{3}V_{1b}} \tag{A.1}$$

Base current in link subsystem:

$$I_{b2} = \frac{S_b}{\sqrt{3}V_{2b}} \tag{A.2}$$

Base current in DC subsystem:

$$I_{db} = \frac{S_b}{V_{db}} \tag{A.3}$$

Base impedance in AC subsystem:

$$Z_{b1} = \frac{V_{1b}^2}{S_b} \tag{A.4}$$

Base impedance in link subsystem:

$$Z_{b2} = \frac{V_{2b}^2}{S_b} \tag{A.5}$$

Base impedance in AC subsystem:

$$Z_{db} = \frac{V_{db}^2}{S_b} \tag{A.6}$$

where

R is the line resistance

X is the line reactance

where

S_n is rated power of power transformer

V_1 is rated voltage of power transformer primary side

Table A.2: AC line parameters

Number	From	To	R (Ohm/m)	X (Ohm/m)
1	1	2	7.21249	37.24256
2	1	4	7.69066	39.71168
3	1	6	6.47530	33.43600
4	2	5	1.99240	10.28800
5	3	4	4.00472	20.67888
6	3	5	1.89278	9.77360

Table A.3: DC line parameters

Number	From	To	R (Ohm/m)
1	1	2	0.59
2	2	3	1.18
3	2	4	0.354
4	3	4	0.59

Table A.4: Link line parameters

No.	DC node (from)	AC node (To)	Sn (VA)	V1 (V)	V2 (V)	Pcu (W)	Vcc (%)	Rdiode_on (Ohm)
1	1	2	1315e3	24000	1221	13300	5.5	1e-3
2	3	3	1315e3	24000	1221	13300	5.5	1e-3
3	4	4	1315e3	24000	1221	13300	5.5	1e-3

V_2 is rated voltage of power transformer secondary side

P_{cu} is copper losses

R_{diode_on} is the commutation resistance of the rectifier

Other related parameters can be calculated as following:

Rated current primary side:

$$I_1 = \frac{S_n}{\sqrt{3}V_1} \tag{A.7}$$

Rated current secondary side:

$$I_2 = \frac{S_n}{\sqrt{3}V_2} \tag{A.8}$$

Transformer short circuit impedance:

$$Z_{cc\_t} = \frac{V_1^2 V_{cc}}{100 S_n} \tag{A.9}$$

Transformer short circuit resistance:

$$R_{cc\_t} = \frac{P_{cu}}{3I_1^2} \tag{A.10}$$

Transformer short circuit resistance:

$$X_{cc\_t} = \sqrt{Z_{cc\_t}^2 - R_{cc\_t}^2} \tag{A.11}$$

Grid impedance:

$$Z_{eq} = \frac{V_2^2}{S_{cc}} \tag{A.12}$$

Commutation impedance:

$$Z_{eq\_total} = Z_{eq} + Z_{cc} + R_{diode\_on} \tag{A.13}$$

Table A.5: AC node parameters

No.	Type	Vd (V)	Vq (V)	P (W)	Q (VAr)
1	Slack	25000	0	0	0
2	PQ	0	0	0	0
3	PQ	0	0	0	0
4	PQ	0	0	0	0
5	PQ	0	0	400000	0
6	PQ	0	0	1000000	800000

where

V_d is d axis voltage

V_q is q axis voltage

P is active power

Q is reactive power

Bibliography

[1] P. Wu and Q. Wang, "Research of the automatic train stop control based on adaptive generalized predictive control," Control Conference (CCC), 2014 33rd Chinese, Nanjing, 2014, pp. 3399-3404.

[2] W. ShangGuan, X. H. Yan, B. G. Cai and J. Wang, "Multiobjective Optimization for Train Speed Trajectory in CTCS High-Speed Railway With Hybrid Evolutionary Algorithm," in IEEE Transactions on Intelligent Transportation Systems, vol. 16, no. 4, pp. 2215-2225, Aug. 2015.

[3] V. Calderaro, V. Galdi, G. Graber, A. Piccolo and D. Cogliano, "An algorithm to optimize speed profiles of the metro vehicles for minimizing energy consumption," Power Electronics, Electrical Drives, Automation and Motion (SPEEDAM), 2014 International Symposium on, Ischia, 2014, pp. 813-819.

[4] N. Bešinovic, E. Quaglietta and R. M. P. Goverde, "Calibrating dynamic train running time models against track occupation data using simulation-based optimization?," 16th International IEEE Conference on Intelligent Transportation Systems (ITSC 2013), The Hague, 2013, pp. 1041-1046.

[5] Q. Gu, T. Tang and F. Ma, "Energy-Efficient Train Tracking Operation Based on Multiple Optimization Models," in IEEE Transactions on Intelligent Transportation Systems, vol. 17, no. 3, pp. 882-892, March 2016.

[6] X. Xia and J. Zhang, "Modeling and Control of Heavy-Haul Trains [Applications of Control]," in IEEE Control Systems, vol. 31, no. 4, pp. 18-31, Aug. 2011.

[7] L. Zhang and X. Zhuan, "Optimal Operation of Heavy-Haul Trains Equipped With Electronically Controlled Pneumatic Brake Systems Using Model Predictive Control Methodology," in IEEE Transactions on Control Systems Technology, vol. 22, no. 1, pp. 13-22, Jan. 2014.

[8] C. Landi, M. Luiso and N. Pasquino, "A Remotely Controlled Onboard Measurement System for Optimization of Energy Consumption of Electrical Trains," in IEEE Transactions on Instrumentation and Measurement, vol. 57, no. 10, pp. 2250-2256, Oct. 2008.

[9] M. Natkin, Automatic train control using neuro-fuzzy modeling and optimal control techniques, Ph.D. dissertation, Kate Gleason College of Engineering, Apr. 1996.

[10] Jinling Zhu, Xiaoyun Feng, Qing He and Jian Xiao, "The simulation research for the ATO model based on fuzzy predictive control," Proceedings Autonomous Decentralized Systems, 2005. ISADS 2005., 2005, pp. 235-241.

[11] H. Oshima, S. Yasunobu and S. i. Sekino, "Automatic train operation system based on predictive fuzzy control," Artificial Intelligence for Industrial Applications, 1988. IEEE AI '88., Proceedings of the International Workshop on, Hitachi City, Japan, 1988, pp. 485-489.

[12] B. P. Rochard and F. Schmid, "A review of methods to measure and calculate train resistances", Proceedings of the Institution of Mechanical Engineers, Part F: Journal of Rail and Rapid Transit, vol. 214, no. 4, pp. 185–199, 2000.

[13] G. Boschetti, A. Mariscotti, "The parameters of motion mechanical equations of a source of uncertainty for traction systems simulation", XX IMEKO World Congress Metrology for Green Growth September 9 to 14, 2012, Busan, Republic of Korea

[14] Muhammad Umer Nawaz, "Estimation of Running Resistance in Train Tunnels", Doctorate thesis, Department of Production and Quality Engineering, Norwegian University of Science and Technology.

[15] Eduardo Pilo de la Fuente, "Diseño óptimo de la electrificación de ferrocarriles de alta velocidad (Optimal design of the electrification of high-speed railways)", doctorate thesis, Escuela Técnica Superior de Ingeniería, universidad pontificia comillas de Madrid.

[16] S. Su, T. Tang and C. Roberts, "A Cooperative Train Control Model for Energy Saving," in IEEE Transactions on Intelligent Transportation Systems, vol. 16, no. 2, pp. 622-631, April 2015.

[17] Y. Wang, B. De Schutter, B. Ning, N. Groot and T. J. J. van den Boom, "Optimal trajectory planning for trains using mixed integer linear programming," 2011 14th International IEEE Conference on Intelligent Transportation Systems (ITSC), Washington, DC, 2011, pp. 1598-1604.

[18] Y. Wang, B. De Schutter, T. van den Boom and B. Ning, "Optimal trajectory planning for trains under a moving block signaling system," Control Conference (ECC), 2013 European, Zurich, 2013, pp. 4556-4561.

[19] Q. Gu, T. Tang and F. Ma, "Energy-Efficient Train Tracking Operation Based on Multiple Optimization Models," in IEEE Transactions on Intelligent Transportation Systems, vol. 17, no. 3, pp. 882-892, March 2016.

[20] A. Albrecht, P. Howlett, P. Pudney and X. Vu, "Optimal train control: Analysis of a new local optimization principle," Proceedings of the 2011 American Control Conference, San Francisco, CA, 2011, pp. 1928-1933.

[21] P. Wu and Q. Wang, "Research of the automatic train stop control based on adaptive generalized predictive control," Control Conference (CCC), 2014 33rd Chinese, Nanjing, 2014, pp. 3399-3404.

[22] P. G. Howlett, "Optimal strategies for the control of train," Automatica, vol. 32, no. 4, pp. 519–532, Apr. 1996.

[23] P. G. Howlett, P. J. Pudney, and X. Vu, "Local energy minimization in optimal train control," Automatica, vol.45, no. 11, pp. 2692–2698, Nov. 2009

[24] K. K. Wong and T. K. Ho, "Dynamic coast control of train movement with genetic algorithm,"Int. J. Syst. Sci., vol. 35, no. 13, pp. 835–846, Oct. 2004.

[25] B. R. Ke, C. L. Lin and C. C. Yang, "Optimisation of train energy-efficient operation for mass rapid transit systems," in IET Intelligent Transport Systems, vol. 6, no. 1, pp. 58-66, March 2012.

[26] M. Miyatake and K. Matsuda, "Energy saving speed and charge/discharge control of a railway vehicle with On—Board energy storage by means of an optimization model,"IEEJ Trans. Elect. Electron. Eng., vol. 4, no. 6, pp. 771–778, Nov. 2009.

[27] M. Miyatake and H. Ko, "Optimization of train speed profile for minimum energy consumption,"IEEJ Trans. Elect. Electron. Eng., vol. 5, no. 3, pp. 263–269, May 2010.

[28] X. Zhou and M. Zhong, "Single-track train timetabling with guaranteed optimality: Branch-and-bound algorithms with enhanced lower bounds," Transport. Res. B - Meth., vol. 41, pp.320-341, March 2007.

[29] A. D'Ariano, M. Pranzo and I. A. Hansen, "Conflict Resolution and Train Speed Coordination for Solving Real-Time Timetable Perturbations," in IEEE Transactions on Intelligent Transportation Systems, vol. 8, no. 2, pp. 208-222, June 2007.

[30] M. A. Shafia, M. Pourseyed Aghaee, S. J. Sadjadi and A. Jamili, "Robust Train Timetabling Problem: Mathematical Model and Branch and Bound Algorithm," in IEEE Transactions on Intelligent Transportation Systems, vol. 13, no. 1, pp. 307-317, March 2012.

[31] F. Corman, A. D'Ariano, D. Pacciarelli, and M. Pranzo, "A tabu search algorithm for rerouting trains during rail operations," Transport. Res. B - Meth., vol. 44, pp. 175-192, January 2010.

[32] A. Caprara, M. Monaci, P. Toth, and P. L. Guida, "A Lagrangian heuristic algorithm for a real-world train timetabling problem," Discrete Appl. Math., vol. 154, pp. 738-753, April 2006.

[33] S. Mu and M. Dessouky, "Scheduling freight trains traveling on complex networks," Transport. Res. B - Meth., vol. 45, pp. 1103-1123, August 2011.

[34] L. Chen, F. Schmid, M. Dasigi, B. Ning, C. Roberts, and T. Tang, "Realtime train rescheduling in junction areas," Proc. IMechE, Part F: J. Rail and Rapid Transit, vol. 224, pp. 547-557, November 2010.

[35] F. Li, Z. Gao, K. Li, and L. Yang, "Efficient scheduling of railway traffic based on global information of train," Transport. Res. B - Meth., vol. 42, pp. 1008-1030, December 2008.

[36] Y. Zhou, X. Yang, Q. Liu and Z. Zhang, "Train movement high-level model for real-time safety justification and train scheduling based on model predictive control," Intelligent Rail Transportation (ICIRT), 2013 IEEE International Conference on, Beijing, 2013, pp. 48-53.

[37] P. Wang, Y. Zhou, J. Chen, Y. Wang and P. Wu, "Real-Time Train Scheduling and Control Based on Model Predictive Control," 2010 Second WRI Global Congress on Intelligent Systems, Wuhan, 2010, pp. 47-50.

[38] Available at www.abb.com.

[39] Pablo Arboleya Arboleya, "Power systems for electrical transportation", class lecture, University of Oviedo, 2015.